

**CYLINDRICAL DETECTOR AND PREAMPLIFIER DESIGN FOR DETECTING
NEUTRONS**

A Dissertation

by

ZHENGHUA XIA

Submitted to the Office of Graduate Studies of
Texas A&M University
in partial fulfillment of the requirements for the degree of

DOCTOR OF PHILOSOPHY

December 2008

Major Subject: Nuclear Engineering

CYLINDRICAL DETECTOR AND PREAMPLIFIER DESIGN FOR DETECTING
NEUTRONS

A Dissertation
by
ZHENGHUA XIA

Submitted to the Office of Graduate Studies of
Texas A&M University
in partial fulfillment of the requirements for the degree of

DOCTOR OF PHILOSOPHY

Approved by:

Chair of Committee,	Leslie A. Braby
Committee Members,	Warren D. Reece
	John R. Ford
	Michael A. Walker
Head of Department,	Raymond Juzaitis

December 2008

Major Subject: Nuclear Engineering

ABSTRACT

Cylindrical Detector and Preamplifier Design for Detecting Neutrons. (December 2008)

Zhenghua Xia, B.Eng., Tsinghua University;

M.S., University of Cincinnati

Chair of Advisory Committee: Dr. Leslie A. Braby

Tissue equivalent proportional counters are frequently used to measure dose and dose equivalent in mixed radiation fields that include neutrons; however, detectors simulating sites $1\mu\text{m}$ in diameter underestimate the quality factor, Q, for low energy neutrons because the recoil protons do not cross the detectors. Proportional counters simulating different site-sizes can be used to get a better neutron dose equivalent measurement since the range and stopping power of protons generated by neutrons in the tissue-equivalent walls depend on the energy of the primary neutrons. The differences in the spectra measured by different size detectors will provide additional information on the incident neutron energy.

Monte Carlo N-particle extended (MCNPX) code was used to simulate neutron transportation in proportional counters of different simulated tissue diameter. These Monte Carlo results were tested using two solid walled tissue equivalent proportional counters, 2mm and 10mm in diameter, simulating tissue volumes $0.1\mu\text{m}$ and $0.5\mu\text{m}$ in diameter, housed in a single vacuum chamber. Both detectors are built with 3mm thick tissue equivalent plastic (A-150) walls and propane gas inside for dose measurement.

Using these two detectors, the spectra were compared to determine the underestimation of y for large detector, and thereby obtain more information of the incident neutron particles.

Based on the MCNPX simulation and experimental results, we can see that the smaller detector produces a larger average lineal energy than the larger detector, which means the larger detector (0.5 μm diameter tissue equivalent size) underestimates the Q value for the low energy neutron, therefore underestimates the effective dose. These results confirm the results of the typical analysis of lineal energy as a function of site size.

ACKNOWLEDGEMENTS

First of all, I would like to thank my advisor, Dr. Leslie Braby, for his sincere guidance and support during my graduate education, as well as his strong encouragement and patience in my whole Ph.D. life. In addition, I would like to express my thanks to Dr. Dan Reece for his endless and sincere technical advice and help at the Nuclear Science Center. Special thanks go to Dr. John Ford and Dr. Michael Walker for their help and support as members of my committee.

I would like to express my great appreciation for all the help I got from all the people who work at NSC. And I would like to thank all the professors and staff in the Nuclear Engineering Department. I would like to thank my family, my friends and especially my husband, Matthew McGinley, for all their tremendous support.

TABLE OF CONTENTS

	Page
ABSTRACT	iii
ACKNOWLEDGEMENTS	v
TABLE OF CONTENTS	vi
LIST OF FIGURES	viii
LIST OF TABLES	x
CHAPTER	
I INTRODUCTION	1
II THEORY	3
II.1 Background	3
II.2 Monte Carlo code	6
II.3 Neutron source and detectors	6
II.3.1 Americium-beryllium source.....	7
II.3.2 Neutron detector.....	7
II.3.2.a The fill gas in neutron detectors	7
II.3.2.b Neutron reaction in the wall	8
III MONTE CARLO SIMULATIONS	11
III.1 Geometry	11
III.2 Neutron source	14
III.3 Input files for MCNPX	15
III.4 Calculations	16
IV EXPERIMENTAL PROTOCOL	21
IV.1 Preamplifiers.....	22
IV.1.1 Design of preamplifiers	23
IV.2 Detectors.....	25
IV.2.1 Electrical design	25
IV.2.2 Mechanical design	27

CHAPTER		Page
	IV.2.2.a Geometry of the detectors.....	27
	IV.2.2.b The gas in the detectors	29
	IV.2.3 Calibration procedure	31
IV.3	Experiment results.....	33
V	CONCLUSIONS AND DISCUSSION	39
	V.1 MCNPX statistical analysis	40
	V.2 Experimental statistical analysis	40
REFERENCES	42
APPENDIX A	43
APPENDIX B	56
VITA	91

LIST OF FIGURES

FIGURE	Page
1 Neutron transportation.....	5
2 Neutron elastic scattering in lab system and center-of-mass system	9
3 Two walled proportional counters simulating neutrons and secondly protons in different site sizes	12
4 Sketch to show relative positions of detectors in the experiment and MCNPX model.....	13
5 Neutron spectrum in MCNPX simulation	14
6 MCNPX ^{241}Am - ^9Be source code.....	15
7 MCNPX geometry code	15
8 The geometry simulation in MCNPX visual edition.....	16
9 $f(y)$ vs y in MCNPX calculation without shielding	17
10 $yf(y)$ vs y in MCNPX calculation without shielding	18
11 $f(y)$ vs y in MCNPX calculation with plastic shielding	19
12 $yf(y)$ vs y in MCNPX calculation with plastic shielding	19
13 $yf(y)$ vs y in MCNPX calculation with plastic shielding	20
14 The composition of detectors, preamplifiers, amplifiers and ADC	21
15 The preamplifier circuit	22
16 The two parts of the preamplifiers	23
17 The incoming signal and the feedback capacitor for the preamplifier	24
18 Basic elements of a proportional counter	26

FIGURE		Page
19	Two different site sized proportional counters	28
20	Vacuum and proportional counters	29
21	Proton stopping power in propane	32
22	The position of the shielding and detectors	33
23	$f(y)$ vs y in the experimental results without shielding	34
24	$yf(y)$ vs y in the experimental results at low gain MCA without shielding.....	35
25	$yf(y)$ vs y in the experimental results without shielding	36
26	$yf(y)$ vs y in the experimental results at low gain MCA with plastic shielding.....	37
27	$yf(y)$ vs y in the experimental results with plastic shielding	38

LIST OF TABLES

TABLE	Page
1 Guidelines for interpreting the relative error R	40

CHAPTER I

INTRODUCTION

Energy deposition in the small volumes simulated by tissue equivalent proportional counters can be used to evaluate the dose and estimate the dose equivalent deposited by neutrons. However, biological evidence suggests that the relative biological effectiveness can be different for different energy neutrons that produce protons with the same stopping power but different energy and range. Because of the transport of energy of secondly protons, it seems likely that some information related to the velocity of the incoming neutrons, as well as the LET of the resulting protons, will be necessary to predict their biological effect.

A multi-detector system is being developed to improve the dose and dose equivalent measurement for neutrons by adding information on recoil proton range. Two proportional counters simulating different size sites are used. It is anticipated that the differences in the spectra measured by these two detectors will provide additional information on the incident neutron velocities.

In order to predict the results of the measurements, Monte Carlo calculations of energy deposition were conducted. MCNPX is a general-purpose Monte Carlo radiation transport code for modeling the interaction of radiation with materials. MCNPX stands for Monte Carlo N-Particle extended. It extends the capabilities of MCNP4C3 to nearly all particle types, to nearly all energies, and to nearly all applications without an additional computational time penalty. MCNPX is fully three-dimensional and time

This dissertation follows the style of Health Physics.

dependent. It utilizes the latest nuclear cross section libraries and uses physics models for particle types and energies where tabular data are not available. Applications range from outer space (the discovery of water on Mars) to deep underground (where radiation is used to search for oil). MCNPX is used for areas including nuclear medicine, nuclear safeguards, accelerator applications, nuclear criticality, and much more (LANL, 2008).

CHAPTER II

THEORY

II.1.Background

Neutrons are responsible for a significant fraction of the effective dose in a wide variety of radiation exposures. They are produced by high energy photon interactions at cancer treatment clinics, by charged particle interactions at charged particle accelerator laboratories or galactic cosmic ray interaction in the earth's atmosphere, and by nuclear power reactors as well as many other sources.

Thorough experimental investigations of the biological effectiveness of neutrons with various spectra, as well as of monoenergetic neutrons, are needed with particular emphasis on those sources of neutrons which are of importance in radiation protection. As discussed above and in the following chapters, the principal reasons for these needs are that:

- (1) a significant number of workers, including people working in space are currently exposed to neutrons in their occupations;
- (2) It is unlikely that an adequate base of human epidemiological data will become available on the effects of neutrons; and
- (3) There is a significant likelihood that principles gained from radiobiological research with neutrons will advance our general understanding of the biological effects of high LET radiation (Casarett et al. 1994).

Neutron radiobiology is an integral part of radiobiology and, therefore, must be studied in the broader context of the overall field (Casarett et al, 1994).

The primary purpose of this research is to get a better estimate of the LET and dose deposited by the protons generated by the incoming neutrons. If the proton stops in the site and the linear energy is obtained by dividing the energy deposited by the mean chord length of the site, as is generally done when analyzing microdosimetry data (Rossi and Zaider 1996), the result will underestimate the dose equivalent.

Different energy protons have different stopping powers. As shown in figure 1, when the protons are generated by the neutrons reacting with the tissue equivalent wall, some will pass through the gas volume simulating a tissue site a few micrometers in diameter, and some will stop in the site. In the latter case, the conventional analysis will underestimate the LET because the chord length distribution for a sphere will overestimate the average path the proton traveled in the site.

For radiation protection the objective is to measure radiation in a way which can be related to the risk of adverse health effects. Even though the dE/dx is the same, the biological effectiveness may be different for different neutron energies; the shielding designed for different energy neutrons should have different physical and engineering characteristics. LET alone may not be an adequate measure of radiation quality. To fully understand health risk it is essential to characterize the neutron energy deposited and the primary neutron energies.

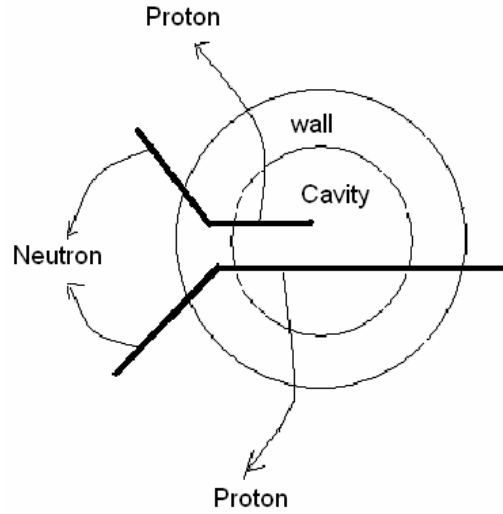


Figure 1. Neutron transportation

The concept of lineal energy, y , is of primary importance to understand the data obtained by a proportional counter. Lineal energy is defined as the quotient of ε by ℓ , where ε is the energy imparted to matter in a volume by a single energy deposition event and ℓ is the mean chord length in that volume (Rossi and Zaider, 1996). Lineal energy is not the same as LET (Linear Energy Transfer). The unrestricted linear energy transfer is equal to the average energy dE which a charged particle loses at a distance dl .

For any convex body, according to the Cauchy theorem, the mean chord length is given by $\ell = 4V/S$ in which V is the volume and S is the surface area. If the body is a sphere with the diameter L or a cylindrical with the same height and diameter, L , the mean chord length is $\ell = 2/3L$.

When neutrons pass through matter, they generate secondary protons. The protons carry away nearly all of energy lost by the primary neutron. For particles with the same dE/dx but different total energy and range, the value of y may become smaller as the site size increases or the proton energy decreases because the range of the protons decreases relative to the site diameter. Thus the lineal energy, y , as a function of site diameter, will be different for different energy neutrons. Based on the difference of the spectra we measure with the different size detectors, an indication of the energy of the neutrons can be obtained.

II.2 Monte Carlo code

The name ‘Monte Carlo’ is a reference to a famous casino in Monaco, where physics researcher Stanislaw Ulam’s uncle would borrow money to gamble. The use of randomness and repetitive nature of interactions in a charged particle track is very similar to the activities which happen in casino. Monte Carlo method has a wide range of application: physics, biology, engineering, finance and other areas.

There are several Monte Carlo codes for ionizing radiation transport: GEANT4, MCNP, MCNPX, FLUKA and so on. MCNPX was picked in this research area because it is user friendly and it extends MCNP4C3 to almost all kinds of particles and the full range of energies without penalty in terms of computing time.

II.3 Neutron source and detectors

In order to see the spectral difference between two different site-size detectors, we need a low energy neutron spectrum. The alpha/neutron reaction in a ^{241}Am - ^{9}Be

source produces a wide range of neutron energies, so ^{241}Am - ^9Be source was picked in this research project.

II.3.1 Americium-beryllium source

Americium is a byproduct of plutonium production activities and the most common isotope is ^{241}Am , an alpha particle emitter. A common neutron source is composed by ^{241}Am and ^9Be . When the ^{241}Am decays and gives off alphas particles, ^9Be will absorb alpha particles and generate neutrons, through the $\text{Be}(\alpha, n)$ reaction. The reaction is shown in the following formula: $^7\text{Be} + ^4\text{He} \rightarrow ^{12}\text{C} + \text{n}$, which has a Q value of 5.71Mev.

II.3.2 Neutron detectors

Proportional counters can be used to detect alpha, beta and neutron activities and to some extent for x-ray spectroscopy. Proportional counters are usually operated in pulse mode since they produce larger pulse than ion chambers. Unlike GM counters, the pulse detected by proportional counters reflects the incoming particle energy deposited in the detector gas.

II.3.2.a. The fill gas in neutron detectors

Two proportional counters are placed in one vacuum chamber to get the same gas pressure and environment. When the charged particle pass through distance d in a specific volume, the energy deposited in this site equals to:

$$E = \frac{dE}{r dX} r d$$

E -----energy deposition in the site size

$\frac{dE}{r dX}$ -----mass stopping power for the target material

ρ -----the density of the target material

d -----the distance the charged particles transported

In order to simulate a tissue equivalent plastic with density ρ_1 and site size d_1 by propane gas with density ρ_2 and site size diameter d_2 , the local energy deposition should be the same, which means

$$\frac{dE_1}{r_1 dX_1} r_1 d_1 = \frac{dE_2}{r_2 dX_2} r_2 d_2$$

During the previous experiments it was found that propane had the good gas gains, energy resolutions and gain stability in proportional counters, so propane was used in our proportional counters. Propane is a three carbon alkane, normally a gas, but compressible to liquid when it is transported. (Propane 2008) The molecular formula is $\text{CH}_3\text{CH}_2\text{CH}_3$.

II.3.2.b.Neutron reaction in the wall

The wall of the neutron detectors is made of A-150 plastic. A-150 tissue equivalent plastic is an electrical conductor and can be used as the cathode of proportional counters. The density of A-150 plastic is 1.127g/cm^3 . The atomic composition of A-150 plastic are 10.1327% hydrogen, 77.5501% carbon, 3.5057% nitrogen, 5.2316% oxygen, 1.7422% fluorine and 1.8378% calcium by weight. Incident neutrons react with the different nuclei in the wall according to their respective cross section. Both inelastic

scattering and elastic scattering are possible for high energy neutrons. In this research most interactions are elastic scattering.

Figure 2 shows the elastic scattering process in the lab system and center-of-mass system.

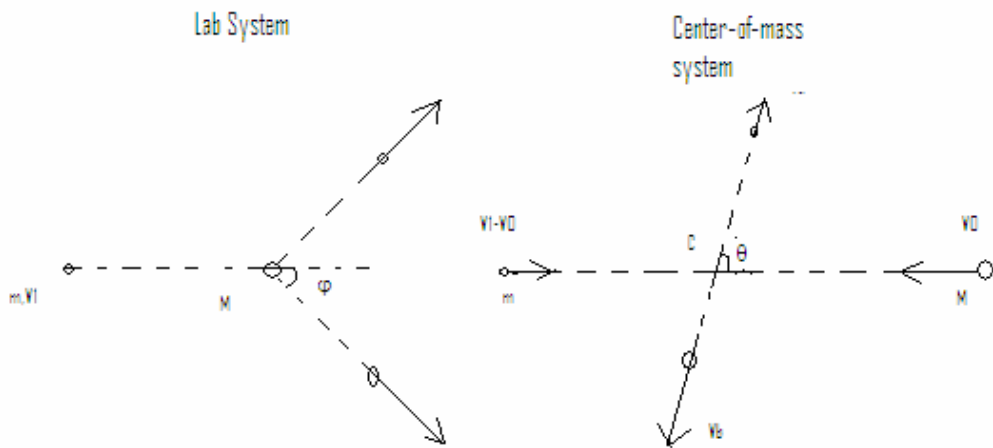


Figure 2. Neutron elastic scattering in lab system and center-of-mass system (Attix 1986)

According to the energy conservation theory, we can get:

$$\frac{E_2}{E_1} = \frac{(m^2 + M^2 + 2mM \cos 2q)}{(m + M)^2}$$

E_2 -----the neutron energy after elastic scattering

E_1 -----the neutron energy before elastic scattering

If α is defined as the mass number of the target, we can get

$$\frac{E_2}{E_1} = 0.5' [(1 + \alpha) + (1 - \alpha) \cos q]$$

From the above formula, we can see E_2 changes as the scattering angle θ changes.

When $\theta=0^\circ$, $E_2=E_I$; when $\theta=180^\circ$, the neutron lost the largest energy, which is αE_I .

Additionally the neutron energy should be between αE_I and E_I . When the target particle is hydrogen, $\alpha=0$ and the neutron may lose all its energy.

The A-150 plastic consists of large portion of hydrogen, and the energy of the recoil protons should be equal to $E_I \cos 2\varphi$. Φ is the scattering angle of the proton. So even the incoming neutron particles are monoenergetic, the recoil proton spectrums may be continuous.

After the secondary protons are generated in the wall, some of them will enter the cavity and ionize the propane gas. In proportional counters, the electrons will come to the anode to cause the output pulse under the influence of a high voltage.

CHAPTER III

MONTE CARLO SIMULATIONS

III.1 Geometry

The objective is to calculate $f(y)$ for situations that can be measured using real proportional counters, both in a laboratory experiment and in a radiation survey instrument.

The neutrons come through the stainless steel vacuum chamber and react with the tissue equivalent A-150 plastic. As a result of elastic scattering, some recoil secondly protons will escape the wall of the A-150 plastic and ionize the propane gas in the proportional counters and deposit energy in the detector site. Figure 3 illustrates the neutron elastic scattering in the wall and proton transportation in the proportional counter. From Figure 3 we can see some protons pass through the whole propane site size in the small detector while they might stop in the propane site size in the large detector.

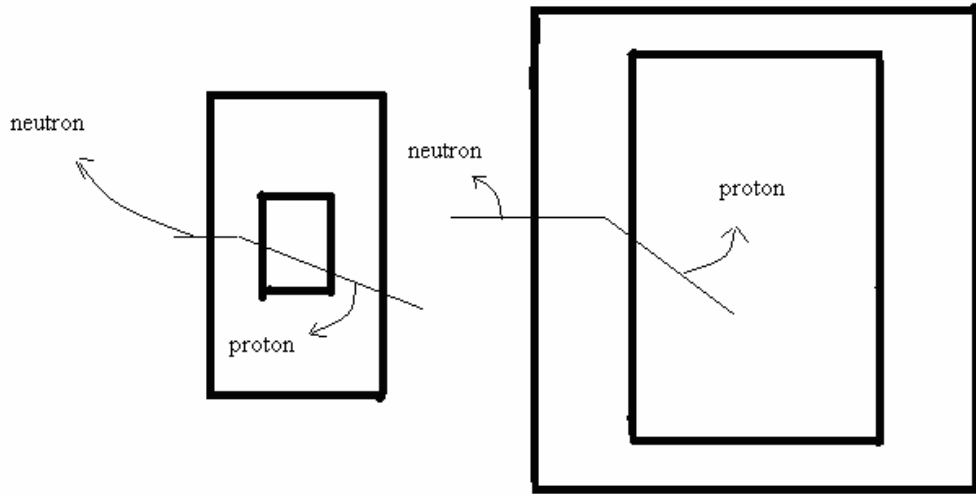


Figure 3. Two walled proportional counters simulating neutrons and secondly protons in different site sizes

The Monte Carlo simulation is close to the real experimental situation, including the position, size and material of the two detectors, gas density and stainless vacuum chamber.

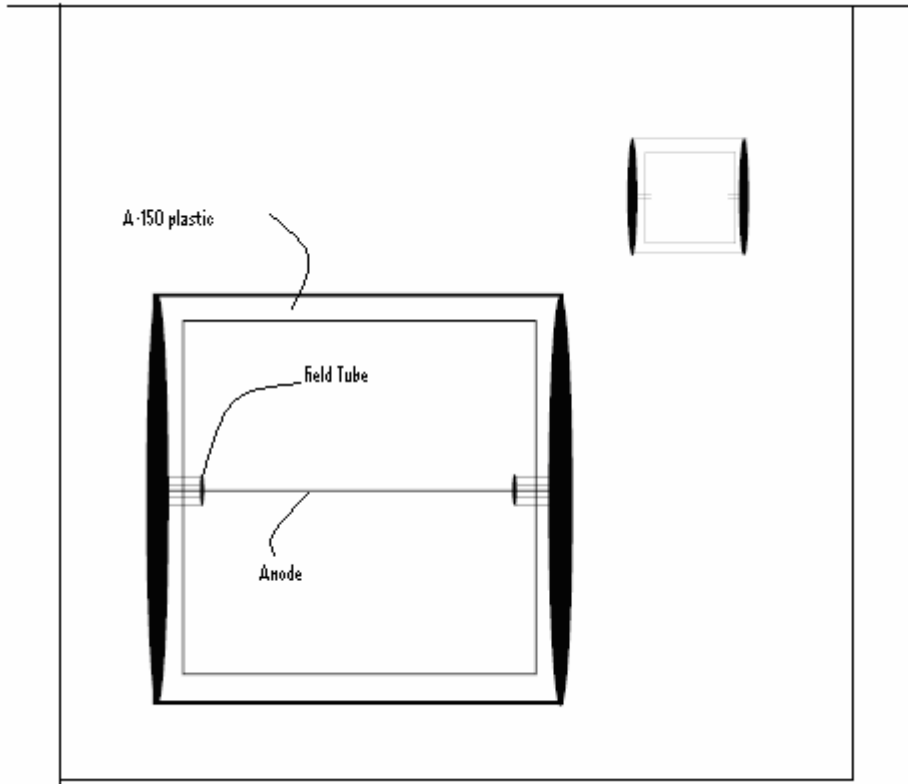


Figure 4. Sketch to show relative positions of detectors in the experiment and MCNPX model

The ratio of the diameters of the detector region of the two detectors is 1:5.

Typical proportional counters are constructed with the cylindrical geometry illustrated in figure 4. The anode consists of a fine wire that is positioned along the axis of a large hollow tube that serves as the cathode. The polarity of the applied voltage in our case will be negative since the high voltage will be connected to the cathode (Knoll 1989).

III.2 Neutron source

^{241}Am - ^9Be source is simulated in MCNPX calculation and the spectrum is illustrated in figure 5. The ^{241}Am in the ^{241}Am - ^9Be source has a long half life, around 433 years, so the source gives the constant neutron fluence rate.

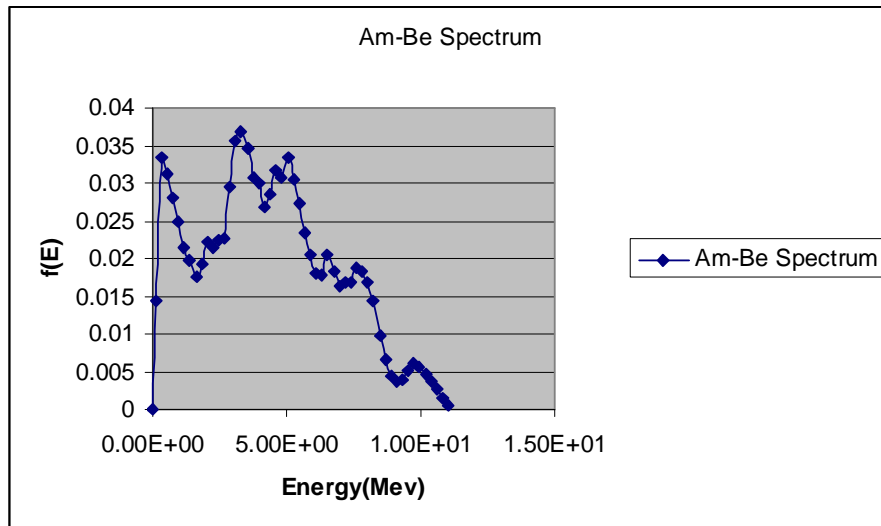


Figure 5. Neutron spectrum in MCNPX simulation

The spectrum in figure 5 is included in standard MCNP files (^{241}Am - ^9Be Spectrum ISO 8529) and was used in the detector simulations. Figure 6 is the MCNPX code for the ^{241}Am - ^9Be source.

```

SI1 H 4.14E-07 0.11 0.33 0.54 0.75 0.97 1.18 1.4 1.61 1.82 2.04&
2.25 2.47 2.68 2.9 3.11 3.32 3.54 3.75 3.97 4.18 4.39 4.61&
4.82 5.04 5.25 5.47 5.68 5.89 6.11 6.32 6.54 6.75 6.96 7.18&
7.39 7.61 7.82 8.03 8.25 8.46 8.68 8.89 9.11 9.32 9.53 9.75&
9.96 10.18 10.39 10.6 10.82 11.03
SP1 D 0 0.0144 0.0334 0.0313 0.0281 0.025 0.0214 0.0198 0.0175&
0.0192 0.0222 0.0215 0.0225 0.0228 0.0295 0.0356 0.0368&
0.0346 0.0307 0.03 0.0269 0.0286 0.0318 0.0307 0.0333 0.0304&
0.0274 0.0233 0.0206 0.0181 0.0177 0.0204 0.0183 0.0163&
0.0168 0.0168 0.0188 0.0184 0.0169 0.0143 0.0097 0.0065&
0.0043 0.0037 0.0038 0.0051 0.0062 0.0055 0.0047 0.0037&
0.0028 0.0015 0.0004 (Roberts 2001)

```

Figure 6. MCNPX ^{241}Am - ^9Be source code

III.3 Input files for MCNPX

The simulation of the geometry in MCNPX is shown in figure 7.

```

c cell card
1 2 -0.000059 -7 -9 10 $large detector
2 2 -0.000059 -13 -15 16 $small detector
3 3 -1.127 (7:9:-10) -11 -8 12 $A150 plastic
4 3 -1.127 (13:15:-16) -17 -14 18 $small detector A150 plastic
5 2 -0.000059 (-12:11:8) (-18:17:14) -1 -3 4
6 4 -8.03 (1:3:-4) -5 -2 6
7 1 -0.00191 (-6:5:2) -19
8 0 19
c surface card
1 cy 2.0
2 cy 2.5
3 py 2.0
4 py -2.0
5 py 2.5
6 py -2.5
7 c/x -1 0 0.5
8 c/x -1 0 0.8
9 px 0.5
10 px -0.5
11 px 0.8
12 px -0.8
13 c/x 0.5 0 0.1
14 c/x 0.5 0 0.4
15 px 0.1
16 px -0.1
17 px 0.4
18 px -0.4
19 so 100
20 pz -8

```

Figure 7. MCNPX geometry code

Although this simulation is very close to the real situation, the fraction of the neutrons that produce protons hitting the detectors is very small. So in order to reduce computing time the simulation was separated into two devices: each detector with its own neutron fluence so a larger fraction of the secondly protons in the small detector will be tracked from the wall to the propane gas. The MCNPX programs are attached in Appendix A.

III.4 Calculations

First, the geometry file was checked by using the MCNP visual editor. Figure 8 is the output from the visual editor.

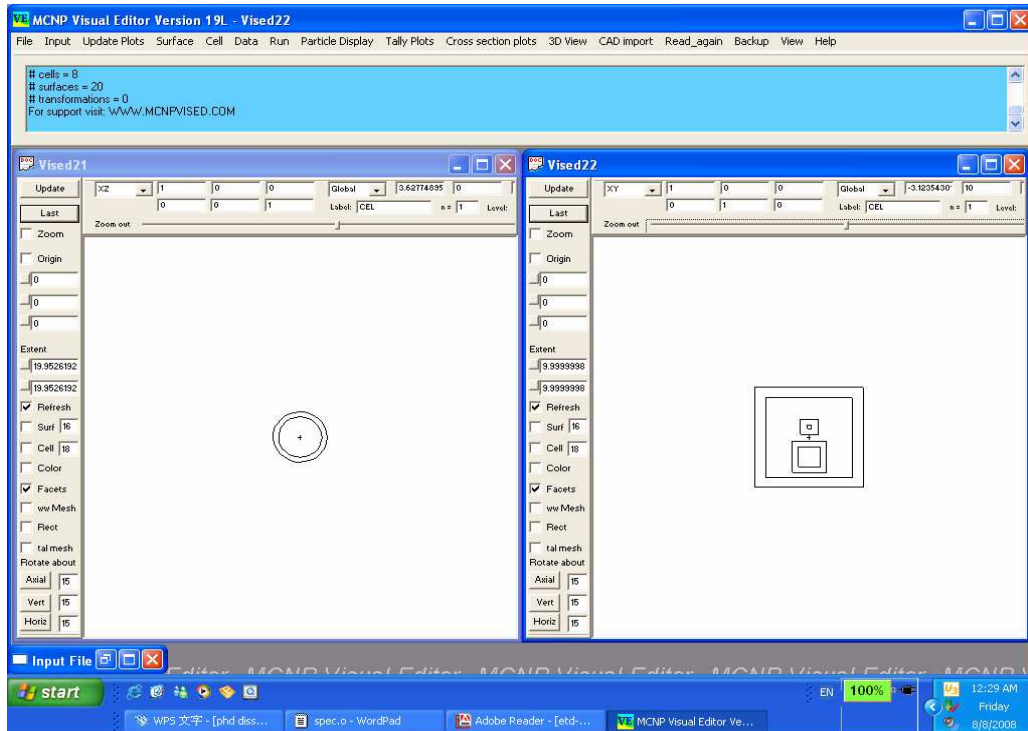


Figure 8. The geometry simulation in MCNPX visual edition

The F8 tally (counts vs deposited energy) for the 10mm diameter detector and 2mm diameter detector are attached in the appendix. F8 tally records the probability versus the deposited energy, which is proportional to the lineal energy. After calibrating the deposited energy to the lineal energy so that it is comparable to the experimental data, the output $f(y)$ vs y spectrum is shown in figure 9. The probability density, $f(y)$, is the probability distribution at different y value. In MCNPX simulation, it was calculated by diving the pulse number at specific y value by the total sum of all the pulses.

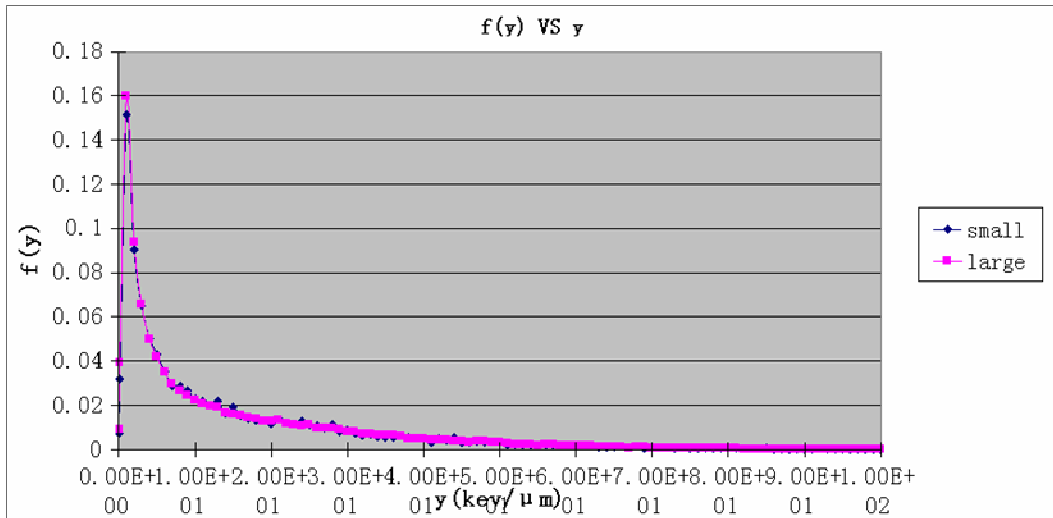


Figure 9. $f(y)$ vs y in MCNPX calculation without shielding

A general feature of most microdosimetric distributions is the fact that both the lineal energy, y , and its distribution, $f(y)$, span a rather large spectrum of values. (Rossi and Zaider 1996) Based on the fact that:

$$f(y)dy = [yf(y)]d\log(y)$$

therefore the area delimited by any two values of y is proportional to the fractional number of events that have lineal energy in that range of y values when $yf(y)$ is plotted against $\log(y)$ (Rossi and Zaider 1996).

Therefore figure 10 was generated to get a better illustration at low y value. Lineal energy is in log scale.

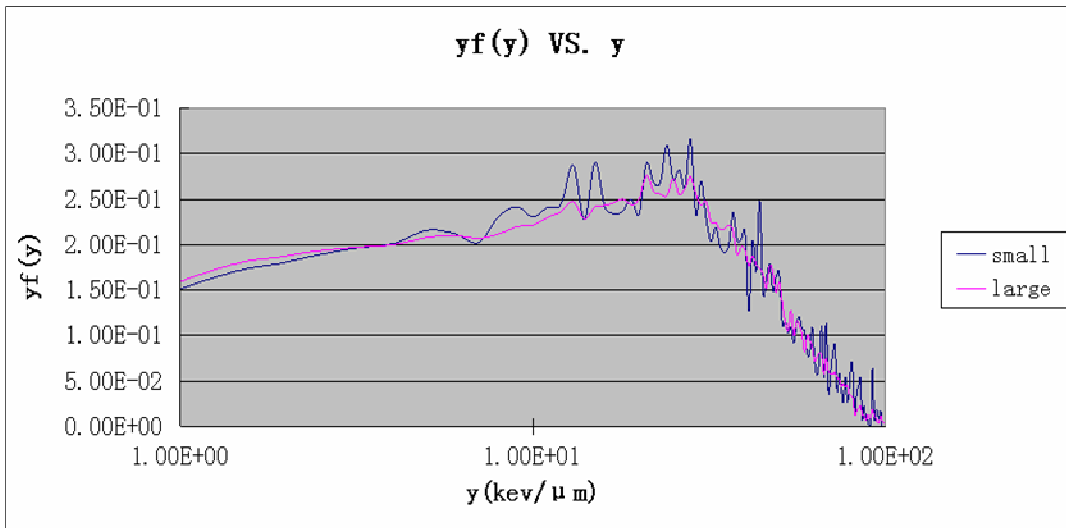


Figure 10. $yf(y)$ vs y in MCNPX calculation without shielding

Since ^{241}Am - ^9Be has a large proportion of high energy neutrons, there is no big difference between the two detectors' spectra. A lower energy neutron spectrum can be produced by placing a plastic shield between the detector and the neutron source. The energy deposition distributions for the two detectors through 2.54cm of polymethyl methacrylate shielding are shown in figure 11 and figure 12.

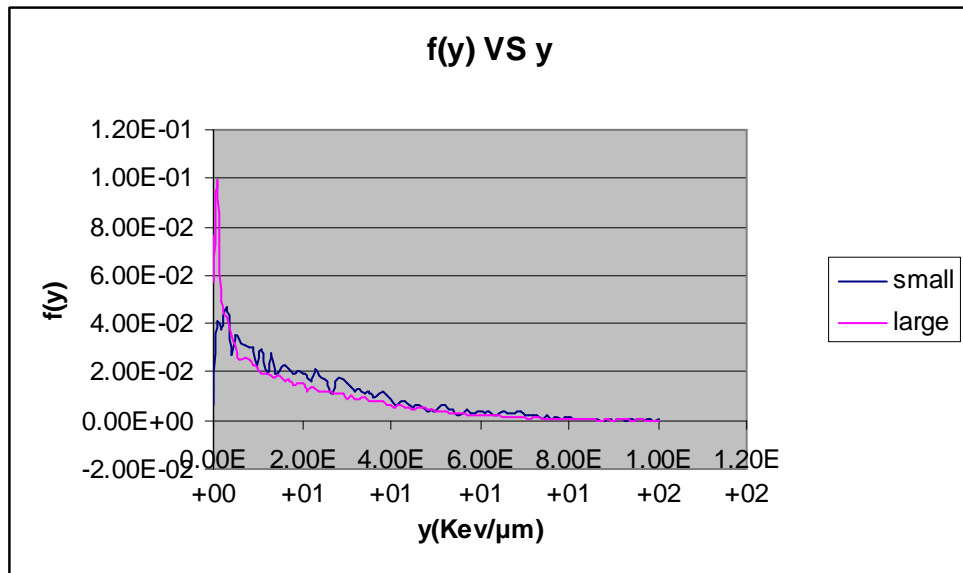


Figure 11. $f(y)$ vs y in MCNPX calculation with plastic shielding

To get a clear comparision between two spectra, $yf(y)$ vs y plot was generated for the MCNPX calculation with a plastic shielding.

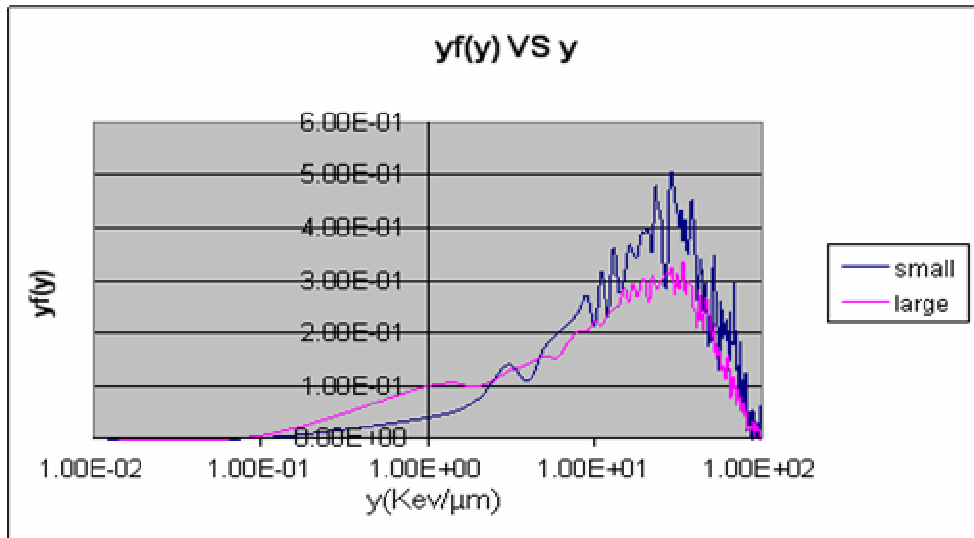


Figure 12. $yf(y)$ vs y in MCNPX calculation with plastic shielding

From figure 11 and figure 12, it is seen that the smaller detector has higher probabilities at large y value (around 100kev μm^{-1}). That means the larger detector will underestimate $f(y)$ for low energy neutrons, therefore Q value for the low energy neutrons will be underestimated in larger detectors.

Figure 13 is the expansion of the spectrum at y value between 1kev μm^{-1} and 100kev μm^{-1} .

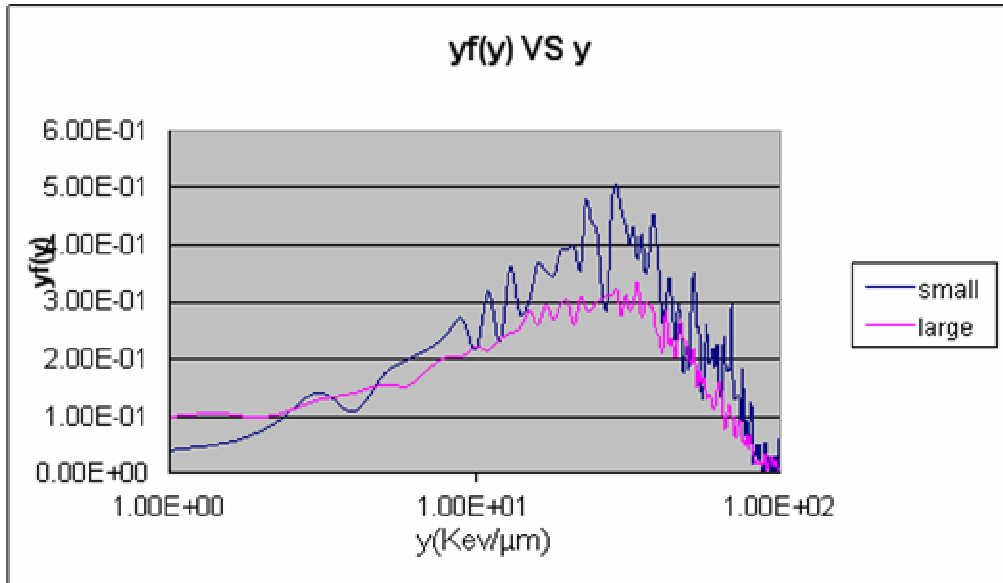


Figure 13. $yf(y)$ vs y in MCNPX calculation with plastic shielding-expand

Since the $^{241}\text{Am}-^9\text{Be}$ source spectrum included in MCNPX doesn't include gamma rays, these calculations do not simulate the low lineal energy events produced by the gamma rays emitted by a real source.

CHAPTER IV

EXPERIMENTAL PROTOCOL

The experiment setup to measure $f(y)$ for neutrons in two simulated sites consists of detector, preamplifier, amplifier, and multichannel analyzer (MCA), which is shown in figure 14:

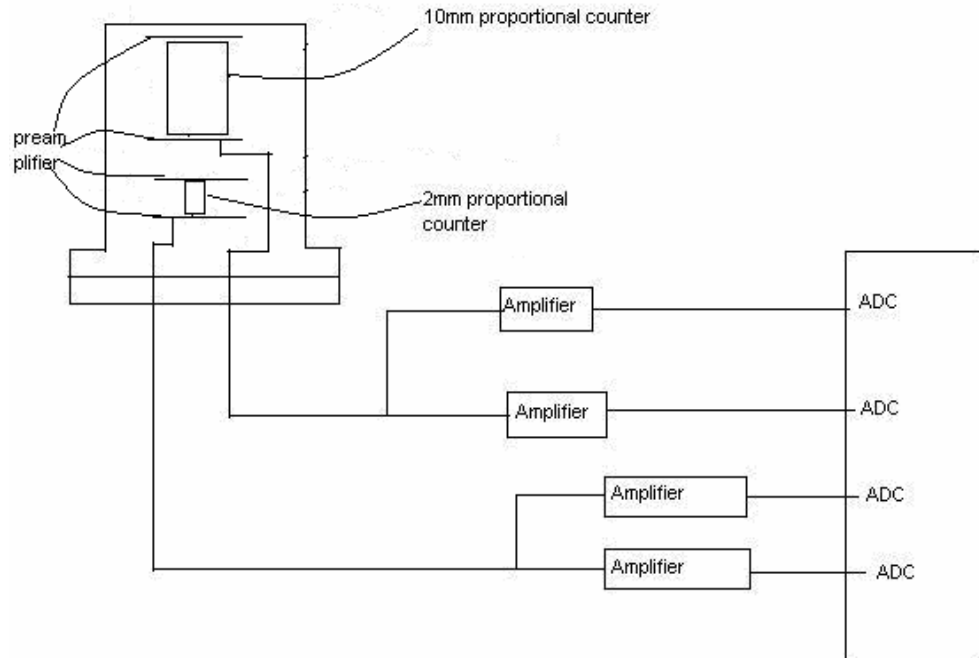


Figure 14. The composition of detectors, preamplifiers, amplifiers and ADC

As shown in figure 14, a single preamplifier is used for each detector. Each preamplifier was built on two printed circuit boards in order to fit conveniently into the vacuum chamber. There are two amplifiers for each detector in order to cover the range of 0-1000kev μm^{-1} with a resolution of about 0.04kev μm^{-1} for events up to 25kev μm^{-1} .

IV.1 Preamplifiers

The diagram of the preamplifier is shown in figure 15. The resistors are in the units of Ω , the capacitors are in the units of μF , and the voltages are in the units of volt. This design was originally developed by Radika (private communication).

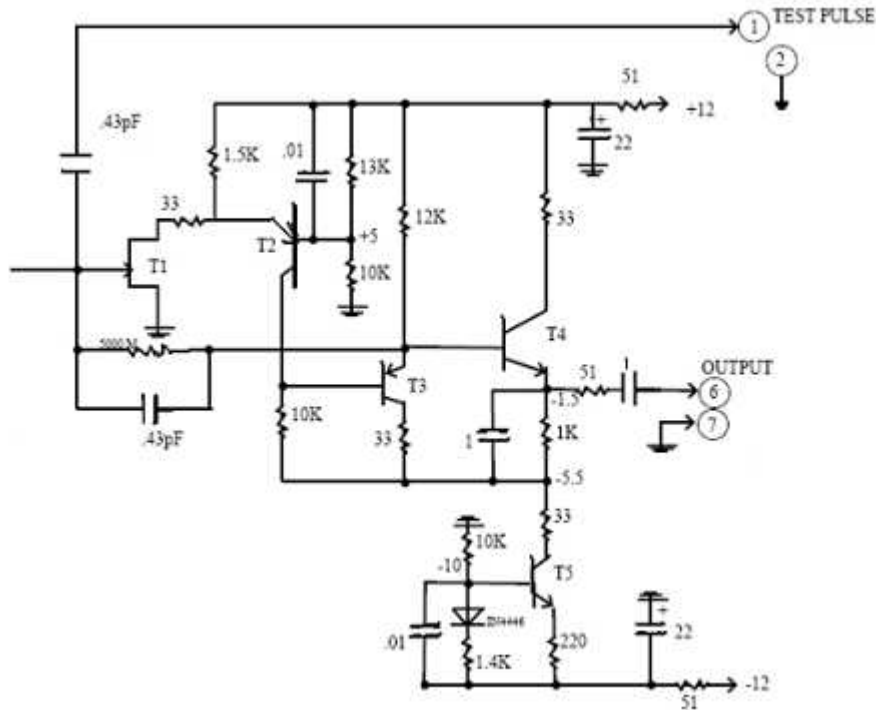


Figure 15. The preamplifier circuit

IV.1.1 Design of preamplifiers

As illustrated in figure 14, the preamplifiers are divided into two parts to be fitted into the vacuum chamber. Figure 16 is the picture of the real two parts of the preamplifiers.



Figure 16. The two parts of the preamplifiers

Eagle software was used to design the circuit boards. Eagle is a schematic capture and printed circuit board design package which is user-friendly and has a freeware version to download. The useable board area for the freeware version is 100*80mm and only two signal layers (top and bottom) can be used.

The feedback and test capacitors are made up of 3 parallel traces on the circuit board as shown in figure 17. The copper lines were made on the rexolite board to decrease the noise. The rexolite board was ordered from C-Lec plastics. The copper was etched by Acu-line Corporation in Washington State.

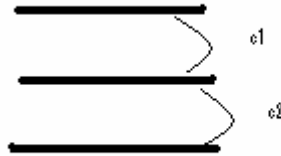


Figure 17. The incoming signal and the feedback capacitor for the preamplifier

In the small detector, $C_1 = 0.6\text{pf}$ and $C_2 = 0.5\text{pf}$. In the large detector, $C_1 = 1.2\text{pf}$ and $C_2 = 1\text{pf}$. The output signal should be similar size of the input signal since the preamplifiers are charge sensitive and the feedback and test capacitors are approximately equal.

The following is how to calculate the noise level for my preamplifier:

For the small detector,

Test pulse voltage $V = 3 \times 10^{-2}\text{V}$

Test capacitor $C = 0.6 \times 10^{-12}\text{F}$

So the total charge is $Q = 1.8 \times 10^{-14}$ Coulombs

In the MCA, the test pulse is in channel 620.

That means $0.3 \times 10^{-16}\text{C}/\text{Channel}$

The noise channel is in channel 6 for the high gain, so if it is converted to the low gain, the noise is: $6/25\text{channels} \times 0.3 \times 10^{-16}\text{C}/\text{Channel} = 7.2 \times 10^{-18}\text{coulombs}$

$1e = 1.6 \times 10^{-19}\text{Coulombs}$

So the noise for the small detector is $7.2 \times 10^{-18}/1.6 \times 10^{-19}\text{electrons} = 50$ electrons

For the large detector,

Test pulse voltage $V = 3 \times 10^{-2} \text{ V}$

Test capacitor $C = 1.2 \times 10^{-12} \text{ F}$

So the total charge is $Q = 3.6 \times 10^{-14} \text{ Coulombs}$

In the MCA, the test pulse is in channel 268.

That means $1.3 \times 10^{-16} \text{ C/Channel}$

The noise channel is in channel 12 for the high gain, so if it is converted to the low gain, the noise is : $12/25 \text{ channels} \times 1.3 \times 10^{-16} \text{ C/Channel} = 6.2 \times 10^{-17} \text{ coulombs}$

$1e = 1.6 \times 10^{-19} \text{ Coulombs}$

So the noise for the large detector is $6.2 \times 10^{-17} / 1.6 \times 10^{-19} = 400 \text{ electrons}$

IV.2 Detectors

IV.2.1 Electrical design

When the distance between the anode and cathode is fixed in a cylindrical detector, the electric field is constant except for end effects. The gas gain is higher for ions produced in the end region (Braby et al. 1995).

The end effect was solved by installing a pair of field tubes on each side of detector in this research project. The field tube is held at a potential which is equal to the voltage that would exist at that surface without the field tubes in an infinitely long cylinder (Braby et al. 1995). Figure 18 shows the basic elements of a proportional counter.

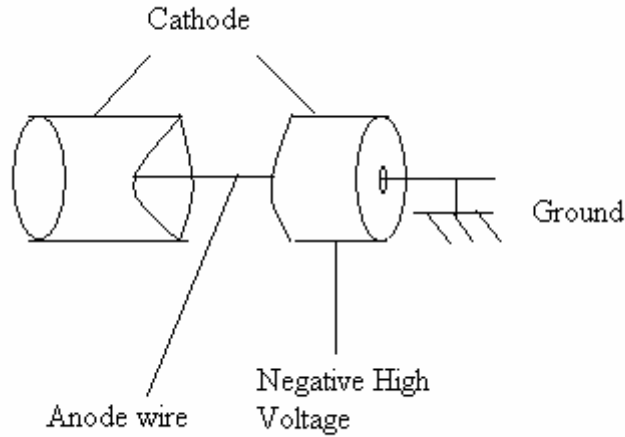


Figure 18. Basic elements of a proportional counter

The electrical field at radius r between the anode and the cathode in figure 18 is:

$$\epsilon(r) = \frac{V}{r \ln(b/a)}$$

Where V = voltage applied between anode and cathode

a = anode wire radius

b = cathode inner radius

r =the distance between the electrical field point to the anode center

In order to keep the electric field constant, the field tube should be connected to the high voltage which will exist at the point without the field tube. In our case, for the small detector:

$$a=0.0005''$$

$$b_1=\text{wall}=0.093''$$

$$b_2=\text{Field Tube}=0.0325''$$

$$\frac{(HV)_{fieldtube}}{HV} = \frac{\ln\left(\frac{0.0325}{0.0005}\right)}{\ln\left(\frac{0.093}{0.0005}\right)} = 80\%$$

So for the voltage divider, the field tube should get 80% of the high voltage for the small detector.

For the large detector:

$$a=0.0005''$$

$$b_1=\text{wall}=0.345\text{ ``}$$

$$b_2=\text{Field Tube}=0.0325\text{ ``}$$

$$\frac{(HV)_{fieldtube}}{HV} = \frac{\ln\left(\frac{0.0325}{0.0005}\right)}{\ln\left(\frac{0.345}{0.0005}\right)} = 64\%$$

So for the voltage divider, the field tube should get 64% of the high voltage for the large detector.

The field tube should be connected to get the right voltage. In this case the field tube for the small detector should get 80% of the high voltage, which is $80\% \times 580 = 464$ volts; the field tube for the large detector should get 64% of the high voltage, which is $64\% \times 600 = 384$ volts.

IV.2.2 Mechanical design

IV.2.2.a Geometry of the detectors

The choice of the detector geometry is the essential first step in the design of a low pressure proportional counter. Detector geometry should be determined primarily by

the requirements of the measurements to be made, but it has a profound effect on both mechanical and electrical design, so some compromises are inevitable. Cylindrical detectors simplify mechanical design as well as electronic design, and may be easier to use in confined spaces.

It is slightly easier to mount the cylindrical detector inside a vacuum chamber, and to make direct connections to the preamplifier because the end of the detector is the full diameter. (Braby et al. 1995)

Materials which are often used for chamber material are aluminum, stainless steel, and plastics. In this research the stainless steel was used to build the vacuum chamber. The detector wall assemblies are shown in figure 19.



Figure 19. Two different size sized proportional counters

The proportional counters and preamplifiers were mounted in a vacuum chamber which is shown in Figure 20.

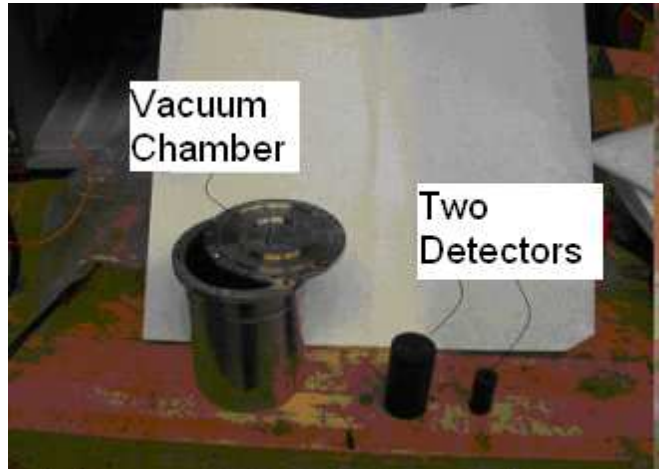


Figure 20. Vacuum and proportional counters

The tissue equivalent plastic serves as the cathode for the detector. Both ends of the wall assembly are connected to the high voltage through a circular copper traces on the preamplifier boards. The anode was made of 25 μm diameter stainless steel wire. In each detector, two springs were soldered on the two parts of the preamplifier boards to give to the tension to keep the anode straight through the detector.

IV.2.2.b The gas in the detectors

The propane gas was picked as the detector gas in this research project. The gain for propane gas doesn't fluctuate as much as it does for tissue equivalent mixtures when the temperature and the water content changes in the environment. Propane doesn't have high electron attachment coefficient, so the gas multiplication, which depends on the free electrons migration, doesn't fluctuate much. The gas was permanently sealed within the vacuum chamber which contains the proportional counters. The vacuum chamber was

sealed by an Indium wire gasket. Indium is a chemical element with chemical symbol In and atomic number 49. This rare, soft, malleable and easily fusible metal makes a very reliable seal between the vacuum chamber and its cover. (Indium 2008)

Two proportional counters are placed in one vacuum chamber to get the same gas pressure and environment. The filling gas pressure is 20 Torr to simulate 0.5 μm with a 10mm diameter detector and 0.1 μm tissue equivalent with a 2mm diameter detector.

In order to simulate a tissue equivalent plastic with density ρ_1 and site size d_1 by propane gas with density ρ_2 and site size diameter d_2 , the local energy deposition should be the same, which means

$$\frac{dE_1}{r_1 dX_1} r_1 d_1 = \frac{dE_2}{r_2 dX_2} r_2 d_2$$

The mass stopping power for the tissue equivalent and propane gas are approximately the same, so we can get $\rho_1 d_1 = \rho_2 d_2$.

In this research project, the gas pressure can be calculated in the following way. In order to simulate 0.1 μm tissue equivalent by 2mm diameter, the propane gas density should be

$$r_1 = \frac{p_2 d_2}{d_1}$$

($\rho_2 = 1\text{g/cm}^3$, $d_2 = 10-4\text{mm}$, $d_1 = 2\text{mm}$). That means the propane density should be $5 \times 10^{-5} \text{ g cc}^{-1}$. The density of an ideal gas is equivalent to $22.4 \text{ liters mole}^{-1}$ at standard temperature and pressure. Propane molecular weight is 44g mole^{-1} . So the density of propane at standard temperature and pressure is

$$\frac{44\text{g}}{22.4\text{liters}} = \frac{11\text{g}}{22.5 \times 10^3 \text{cc}} = 2 \times 10^{-3} \text{ g/cc}$$

at 760 torr. The pressure should be

$$P = \frac{5 \times 10^{-5}}{2 \times 10^{-3}} \text{ atm} = 2.5 \times 10^{-2} \text{ atm} = 18.8 \text{ torr}$$

to get the right simulation in this research case.

IV.2.3 Calibration procedure

The calibration was made based on the test pulse. First to test the multichannel analyzer the input pulses of 2mV, 4mV and 8mV were used. We changed the LLD and ADC conversion gain to get the pulse in reasonable size and to ensure that the channel number is proportional to the input pulse size. The test pulse will show up at one single channel in multichannel analyzer.

To calibrate the MCA, we identify the largest channel where the counts drop as the proton drop point, which is $100\text{kev } \mu\text{m}^{-1}$ for tissue equivalent materials. Proton drop point is the signal produced when the proton has the biggest stopping power, which is shown in figure 21.

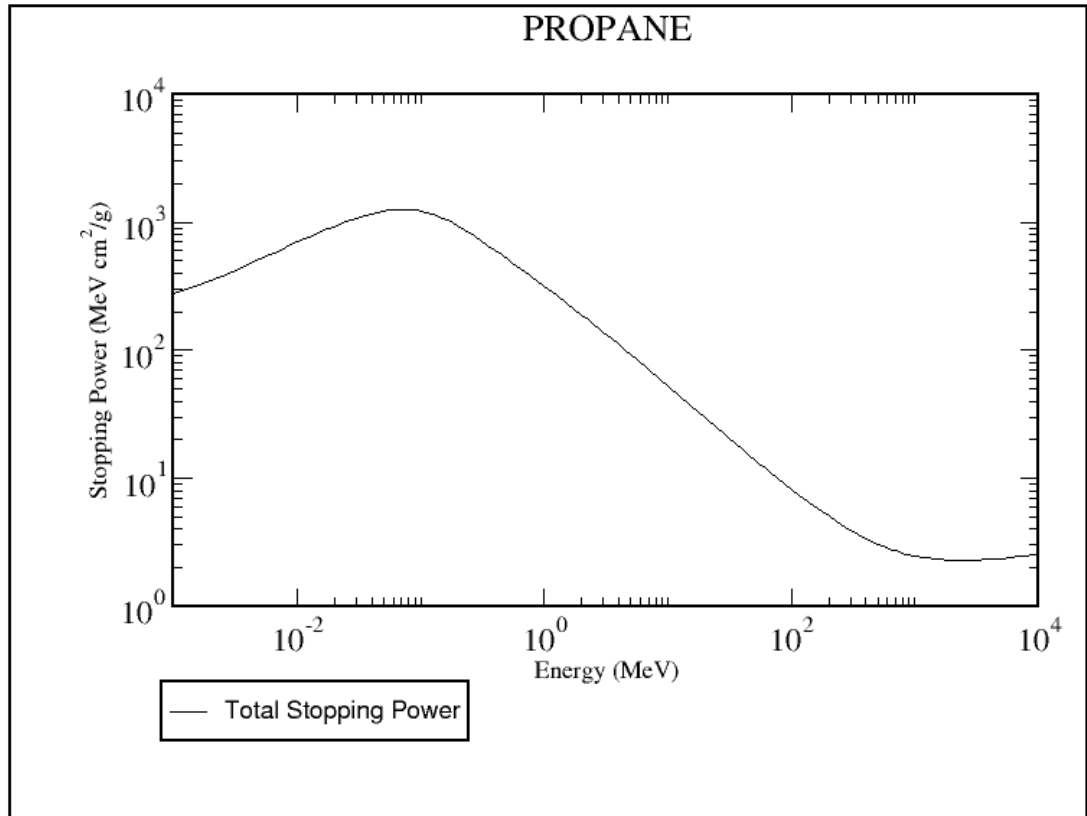


Figure 21. Proton stopping power in propane (NIST 2008)

In this research, the propane is used to simulate tissue, and the highest stopping power of the proton is 1000Mev cm^2/g , which equals $100\text{kev } \mu\text{m}^{-1}$.

The high voltage for the small detector was set at 580V and the high voltage for the large detector was set at 600V. For the proton drop point, at low gain MCA level, the channel corresponding to the maximum energy deposition by a proton, for the small detector, was 100 and the corresponding channel for the large detector was 200. Since the proton drop point happens when the stopping power is $100\text{kev } \mu\text{m}^{-1}$, in which case the lineal energy is $150\text{kev } \mu\text{m}^{-1}$. So the calibration factor for the small detector is 1.5

and the calibration factor for the large detector is $0.75\text{kev } \mu\text{m}^{-1}$ channel for the low gain. The high gain was set at 25 times the low gain, so the high gain resolution was $60\text{ev } \mu\text{m}^{-1}$ channel $^{-1}$ for the small detector and $30\text{ev } \mu\text{m}^{-1}$ channel for the large detector.

IV.3 Experiment results

The $^{241}\text{Am}-^9\text{Be}$ source is a cylindrical source and the detector is 5cm away from the source. The position of the source, shielding and detector is as shown in figure 22.

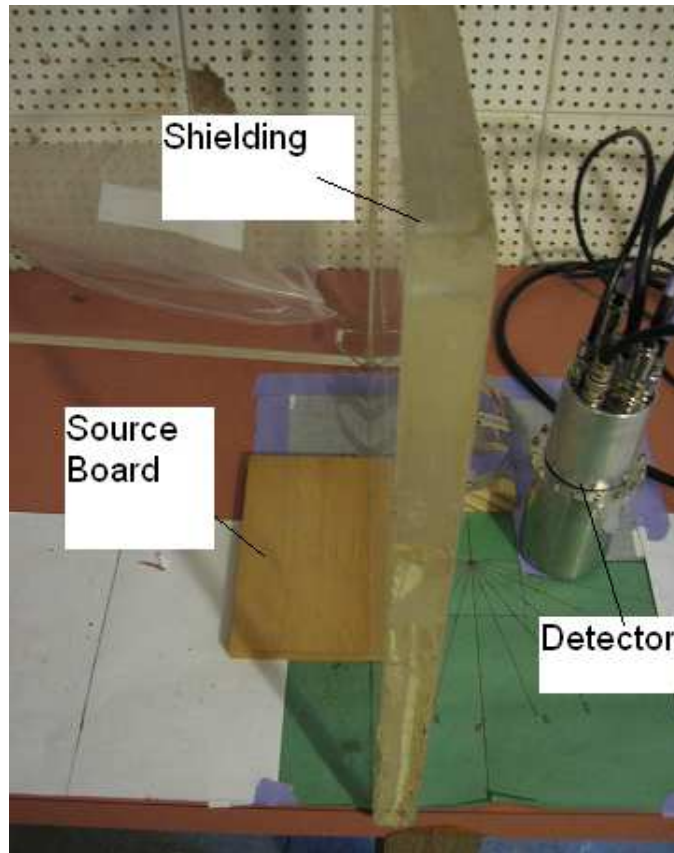


Figure 22. The position of the shielding and detectors

Figures 23, 24 and 25 are experimental results without the plastic shielding.

Figure 23 illustrates $f(y)$ vs y at the low gain part at MCA.

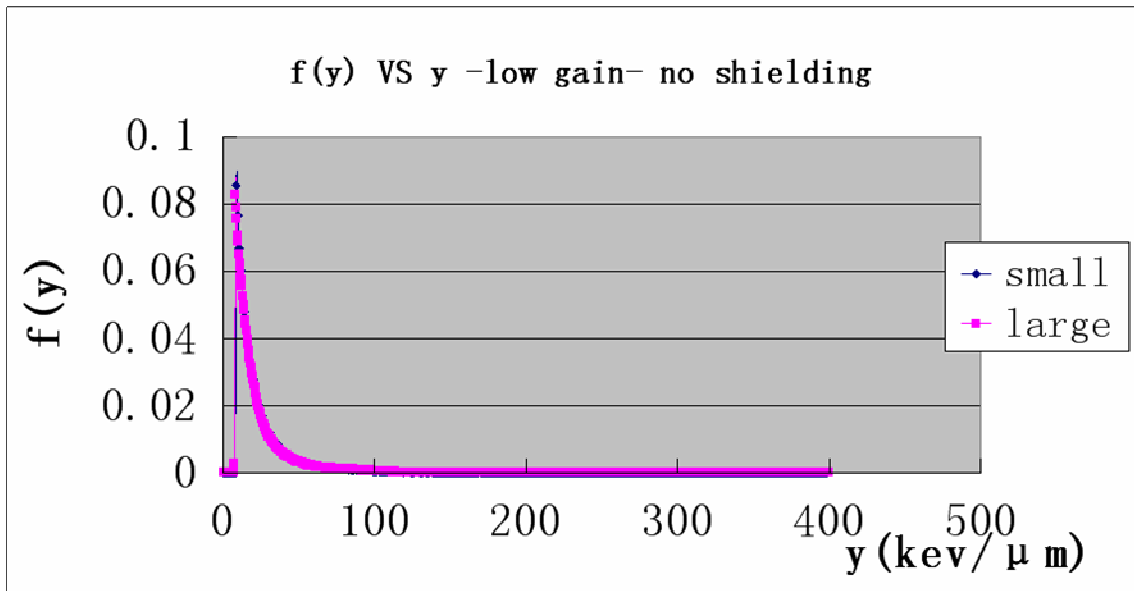


Figure 23. $f(y)$ vs y in the experimental results without shielding

As described in section III.4, if y is in log scale, $yf(y)$ vs y plot is shown in figure 24.

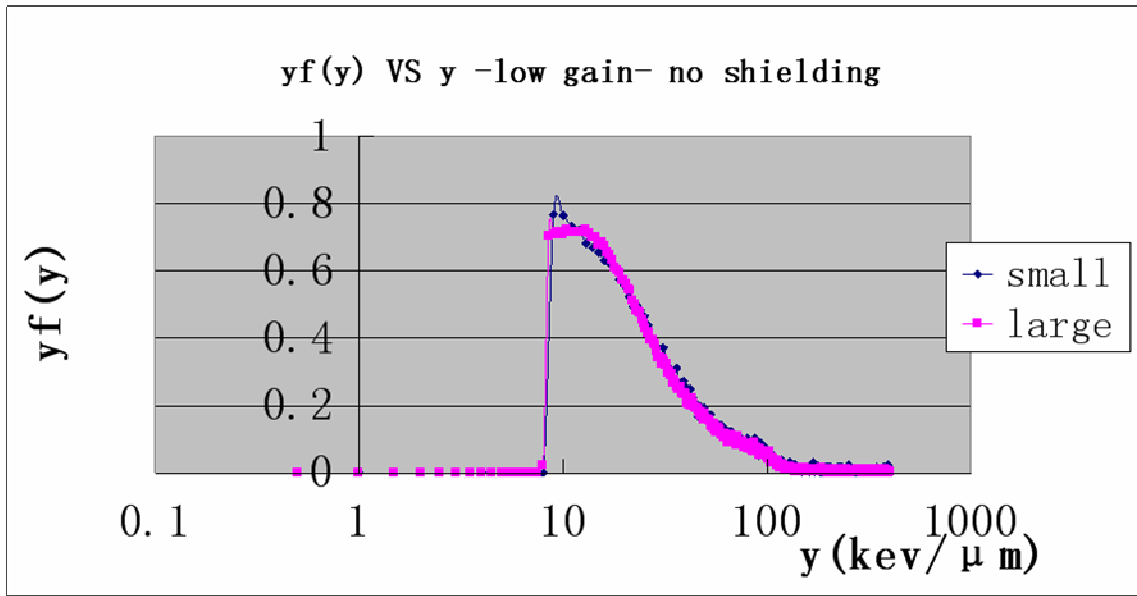


Figure 24. yf(y) vs y in the experimental results at low gain MCA without shielding

If the high gain MCA results are included, which means the counts at y value lower than $10\text{kev } \mu\text{m}^{-1}$ are also included, the distribution in figure 25 is obtained:

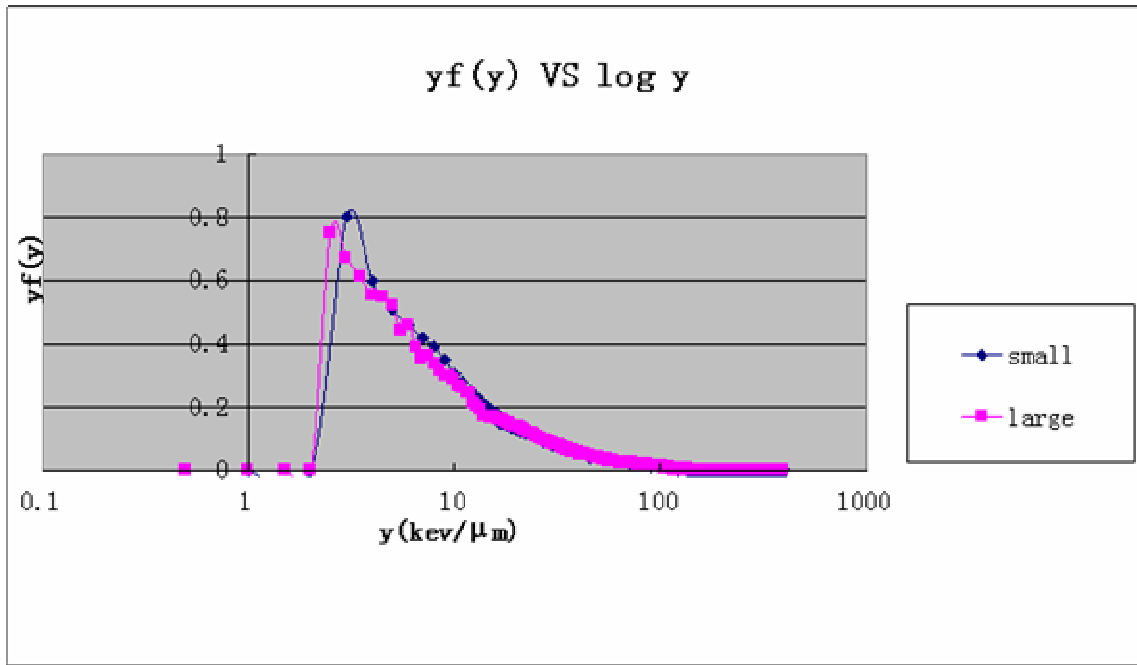


Figure 25. $yf(y)$ vs y in the experimental results without shielding

Figure 23 illustrates the same conclusion as figure 22. Because of differences in dead time in the high gain and low gain data, it was necessary to make a correction of 1.1 to 1.8 in the counts per channel when merging the ghight gain and low gain data for the large detector at y values between $5\text{kev } \mu\text{m}^{-1}$ and $10\text{kev } \mu\text{m}^{-1}$. Since $^{241}\text{Am}-^9\text{Be}$ source has large proportion of high energy neutron, we can not see too much difference between the two detectors spectrums.

After putting a plastic shielding board between the source and the detector, the following two spectra, figure 26 and figure 27 were measured. Figure 26 included the low gain MCA part data.

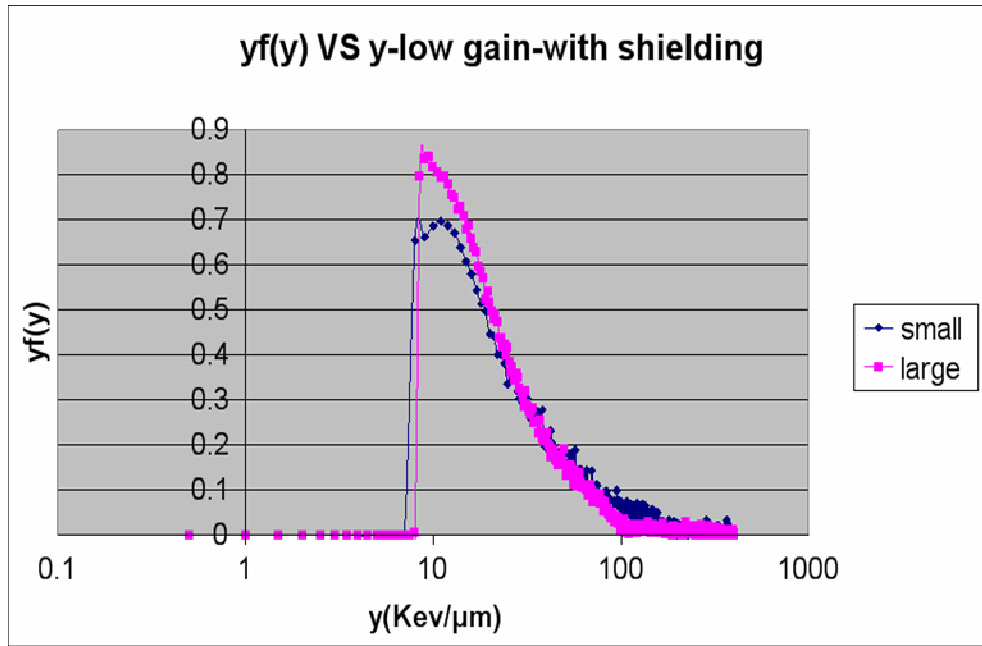


Figure 26. $yf(y)$ vs y in the experimental results at low gain MCA with plastic shielding

From Figure 26, we can see the small detector has more probability of events at large y value (around $100\text{kev } \mu\text{m}^{-1}$), which means the small detector has a bigger average y value. This is more clearly illustrated in the following figure 27.

Figure 27 included the high gain and low gain MCA data.

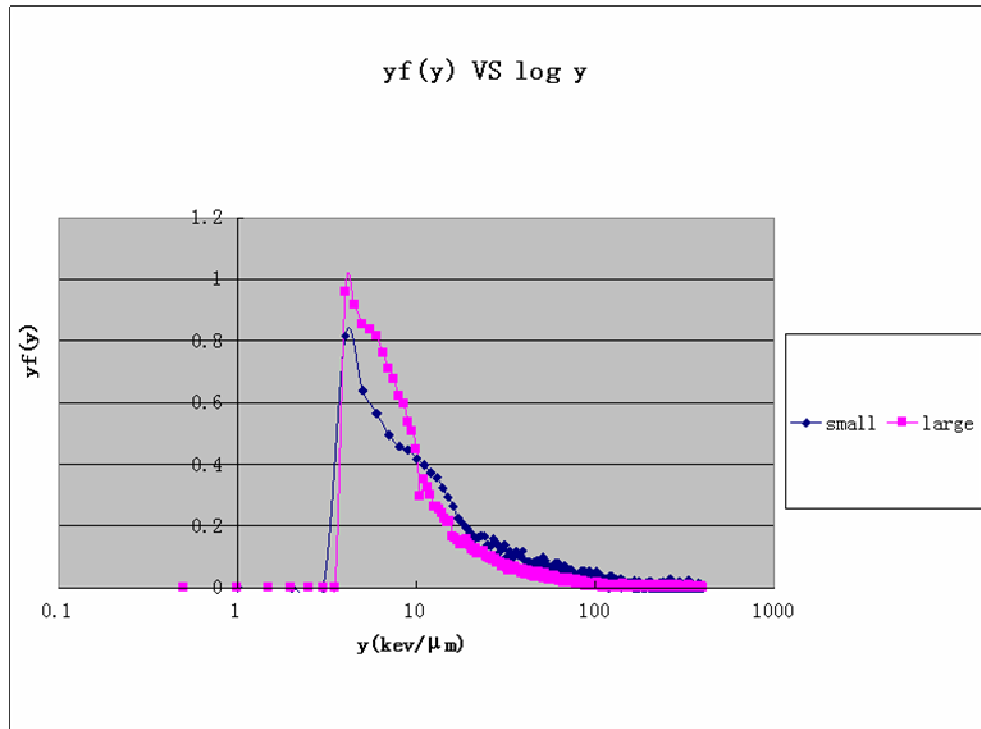


Figure 27. $yf(y)$ vs y in the experimental results with plastic shielding

From figure26 and figure27, we can see the large detector gets higher probability at low y values than the small detector and the small detector has higher probability of large y values. Most neutrons' energy gets smaller after the plastic shielding, which has higher y value (around $100\text{keV } \mu\text{m}^{-1}$). Because of the short range of the low energy neutrons, some neutrons stop in the large detector. In this case the LET is underestimated by dividing the deposited energy by the chord length. From these two figures, we can see the average y value for the small detector is bigger than for the large detector. Therefore the large detector underestimates the Q value and the absorbed dose for the neutron source.

CHAPTER V

CONCLUSIONS AND DISCUSSION

The purpose of this study is to find a way to get a better dose estimation of the low energy neutron dose distribution in a specific site size. Traditional 1 μm site size tissue equivalent proportional counter was proved to underestimate the neutron Q value, therefore underestimate the neutron dose equivalent. Two different site size tissue equivalent proportional counters were made and used to measure the neutron dose distribution in different sizes. MCNPX toolkit was used to simulate the neutron and proton transportation in tissue equivalent plastics and get the theoretical results for the dose distribution in different site sizes.

Based on the MCNPX calculation and experimental results, it was discovered the large detector underestimate LET for low energy protons. LET was estimated by the lineal energy and the lineal energy is smaller than the LET in a large site size. Comparing the spectra between two site size detectors, the feasibility of the site size method was demonstrated.

There is some discrepancy between the MCNPX results and experiment results. One reason is that the Am-Be source in MCNPX simulation doesn't include the gamma source part. Another reason is that MCNPX can't follow more than 1×10^9 tracks in the computer and the statistical error was relatively large. But both experimental and Monte Carlo results were consistant with the site size theory.

V.1 MCNPX statistical analysis

MCNX results were generally reliable when the statistic error is smaller than 0.1 (X-5 Monte Carlo Team 2003). In our calculation, after the modification of the model, the relative error is around 10% for the small detector and 5% for the large detector. Therefore the MCNPX results in this research project are generally reliable. The following table is the standard for deciding if the MCNPX results are reliable.

Table 1. Guidelines for interpreting the relative error R. (X-5 Monte Carlo Team 2003)

Guidelines for Interpreting the Relative Error R	
Range of R	Quality of the Tally
0.5 to 1.0	Not meaningful
0.2 to 0.5	Factor of a few
0.1 to 0.2	Questionable
< 0.10	Generally reliable
< 0.05	Generally reliable for point detectors

V.2 Experimental statistical analysis

For the experimental data, the counts need to be above 100 in the channel we are concerned with getting a statistical error less than 10%. Since the statistic error is obtained from the following formula:

$$R = \frac{1}{\sqrt{N}}$$

Since dead time due to high count rate at low y values limits maximum dose rate during a measurement, several hours may be required to obtain 100 counts at $y=100\text{keV }\mu\text{m}^{-1}$. In this research results, the counts are around 144 at $100\text{kev }\mu\text{m}^{-1}$ for the small detector and the counts are around 287 at $100\text{kev }\mu\text{m}^{-1}$ for the large detector. Therefore the experimental data error is within 10%.

The number of counts in a channel depends on how wide the channel is. The raw data for the large detector has channels $0.5\text{keV }\mu\text{m}^{-1}$ wide, but at $y=100\text{kev }\mu\text{m}^{-1}$, the points overlap each other. At $100\text{keV }\mu\text{m}^{-1}$ resolution of 5 or even $10\text{keV }\mu\text{m}^{-1}$ would be enough to show the curve shape. That is why we normally increase the channel width with increasing y . If 10 channels of data are grouped in one channel, the counting time could be only 1/10 or the time to get the same statistical precision. But several hours are still needed in most cases, especially in the case when the neutron source was in plastic shielding.

Future studies should extend the different site size theory to practical application. Different site size detectors could be made to get a better estimation of low energy neutrons. The theory could also be explored in different particle types to get more accurate dose deposition.

REFERENCES

- Attix FH. Introduction to radiological physics and radiation dosimetry. New York: John Wiley & Sons; 1986.
- Braby LA, Johnson GW, Barthe J. Practical considerations in the design and construction of tissue-equivalent proportional counters. Radiat Protect Dosim 61:351-379; 1995.
- Cadsoft online. Eagle, version 5. Available at: <http://www.cadsoftusa.com/>. Accessed 16 July 2008.
- Casarett GW, Braby LA, Broerse JJ, Elkind MM, Goodhead DT, Oleinick NL. Biological effectiveness of neutrons. Washington, DC: Oak Ridge Associated Universities; 1994.
- Indium. Wikipedia. Available at <http://en.wikipedia.org/wiki/Indium>. Accessed 16 July 2008.
- Knoll GF. Radiation detection and measurement. New York: John Wiley & Sons; 1989.
- Los Alamos National Laboratory (LANL). MCNPX. Available at: <http://mcnpx.lanl.gov/>. Accessed 16 July 2008.
- National Institute of Standards and Technology (NIST). Stopping power and range tables for protons. Available at: http://physics.nist.gov/cgi-bin/Star/ap_table.pl. Accessed 16 July 2008.
- Propane. Wikipedia. Available at <http://en.wikipedia.org/wiki/Propane>. Accessed 16 July 2008.
- Roberts NJ. MCNP calculations of correction factors for radionuclide neutron source emission rate measurements using the manganese bath. NPL Report CIRM 45; 2001.
- Rossi HH, Zaider MS. Microdosimetry and its applications. Berlin: Springer; 1996.
- X-5 Monte Carlo Team. MCNP-a general Monte Carlo N-particle transport code, version 5. MCNP Users Manual 1:7; 2003.

APPENDIX A

MCNPX PROGRAMS AND OUTPUT

Section I. MCNPX input programs

Section I.1 MCNPX simulation for the whole geometry without shielding

```

c cell card
1 2 -0.000059 -7 -9 10 $large detector
2 2 -0.000059 -13 -15 16 $small detector
3 3 -1.127 (7:9:-10) -11 -8 12 $A150 plastic
4 3 -1.127 (13:15:-16) -17 -14 18 $small detector A150 plastic
5 2 -0.000059 (-12:11:8) (-18:17:14) -1 -3 4
6 4 -8.03 (1:3:-4) -5 -2 6
7 1 -0.00191 (-6:5:2) -19
8 0 19

c surface card
1 cy 2.0
2 cy 2.5
3 py 2.0
4 py -2.0
5 py 2.5
6 py -2.5
7 c/x -1 0 0.5
8 c/x -1 0 0.8
9 px 0.5
10 px -0.5
11 px 0.8
12 px -0.8
13 c/x 0.5 0 0.1
14 c/x 0.5 0 0.4
15 px 0.1
16 px -0.1
17 px 0.4
18 px -0.4
19 so 100
20 pz -8

mode n h
IMP:n,h 1 1 1 1 1 1 1 0
nps 1000000
c source definition
SDEF par=1 erg=d1 SUR=20 POS=0 0.5 -8 RAD=d2 ext=d3
SI1 H 4.14E-07 0.11 0.33 0.54 0.75 0.97 1.18 1.4 1.61 1.82 2.04&
2.25 2.47 2.68 2.9 3.11 3.32 3.54 3.75 3.97 4.18 4.39 4.61&
4.82 5.04 5.25 5.47 5.68 5.89 6.11 6.32 6.54 6.75 6.96 7.18&
7.39 7.61 7.82 8.03 8.25 8.46 8.68 8.89 9.11 9.32 9.53 9.75&
9.96 10.18 10.39 10.6 10.82 11.03
SP1 D 0 0.0144 0.0334 0.0313 0.0281 0.025 0.0214 0.0198 0.0175&
0.0192 0.0222 0.0215 0.0225 0.0228 0.0295 0.0356 0.0368&
0.0346 0.0307 0.03 0.0269 0.0286 0.0318 0.0307 0.0333 0.0304&
0.0274 0.0233 0.0206 0.0181 0.0177 0.0204 0.0183 0.0163&
0.0168 0.0168 0.0188 0.0184 0.0169 0.0143 0.0097 0.0065&

```

```

0.0043 0.0037 0.0038 0.0051 0.0062 0.0055 0.0047 0.0037&
0.0028 0.0015 0.0004
SI2 = 0 2
SI3 = 4
F8:n 1
E8 0 48I 12
F18:n 2
E18 0 48I 12
c material specification
M1 006012 -0.02 008016 -0.28 007014 -0.70 $air
M2 001001 -0.7273 006012 -0.2727 $propane c3h8
M3 001001 -0.102 006012 -0.768 008016 -0.0592 007014 -0.036 &
020040 -0.018 009019 -0.017 $A150
M4 028058 -0.09 024050 -0.18 026054 -0.6981 014028 -0.01 012000 -0.02 &
006012 -0.0012 015031 -0.0004 016032 -0.0003 $steel

```

Section I.2 MCNPX simulation for the large detector without shielding

```

Final program 1
c cell card
1 2 -0.000059 -1 -3 4 $large detector propane
2 3 -1.127 (1:3:-4) -2 -5 6 $large detector TEQC
3 1 -0.00191 (2:5:-6) -7 $air
4 0 7 $outside area

c surface card
1 cx 0.5
2 cx 0.8
3 px 0.5
4 px -0.5
5 px 0.8
6 px -0.8
7 so 6
c 8 pz -3

mode n h p
IMP:n,h,p 1 1 1 0
nps 1e9
c source definition
SDEF par=1 erg=d1 POS=0 0 -3 VEC=0 0 1 DIR=1 RAD=d2 ext=0
SI1 H 4.14E-07 0.11 0.33 0.54 0.75 0.97 1.18 1.4 1.61 1.82 2.04&
2.25 2.47 2.68 2.9 3.11 3.32 3.54 3.75 3.97 4.18 4.39 4.61&
4.82 5.04 5.25 5.47 5.68 5.89 6.11 6.32 6.54 6.75 6.96 7.18&
7.39 7.61 7.82 8.03 8.25 8.46 8.68 8.89 9.11 9.32 9.53 9.75&
9.96 10.18 10.39 10.6 10.82 11.03
SP1 D 0 0.0144 0.0334 0.0313 0.0281 0.025 0.0214 0.0198 0.0175&
0.0192 0.0222 0.0215 0.0225 0.0228 0.0295 0.0356 0.0368&
0.0346 0.0307 0.03 0.0269 0.0286 0.0318 0.0307 0.0333 0.0304&
0.0274 0.0233 0.0206 0.0181 0.0177 0.0204 0.0183 0.0163&
0.0168 0.0168 0.0188 0.0184 0.0169 0.0143 0.0097 0.0065&
0.0043 0.0037 0.0038 0.0051 0.0062 0.0055 0.0047 0.0037&
0.0028 0.0015 0.0004
SI2 = 0 0.4
F8:n,h,p 1

```

```

E8 0 1e-5 1e-3 1e-2 0.1 8i 1 89i 10
c material specification
M1 006012 -0.02 008016 -0.28 007014 -0.70 $air
M2 001001 -0.7273 006012 -0.2727 $propane c3h8
M3 001001 -0.102 006012 -0.768 008016 -0.0592 007014 -0.036 &
020040 -0.018 009019 -0.017 $A150

```

Section I.3 MCNPX simulation for the small detector without shielding

```

Final program 1
c cell card
1 2 -0.000059 -1 -3 4 $small detector air
2 3 -1.127 (1:3:-4) -2 -5 6 $small detector TEQC
3 1 -0.00191 (2:5:-6) -7 $air
4 0 7 $outside area

c surface card
1 cx 0.1
2 cx 0.4
3 px 0.1
4 px -0.1
5 px 0.4
6 px -0.4
7 so 6
c 8 pz -3

mode n h p
IMP:n,h,p 1 1 1 0
nps 1e9
c source definition
SDEF par=1 erg=d1 POS=0 0 -3 VEC=0 0 1 DIR=1 RAD=d2 ext=0
SI1 H 4.14E-07 0.11 0.33 0.54 0.75 0.97 1.18 1.4 1.61 1.82 2.04&
2.25 2.47 2.68 2.9 3.11 3.32 3.54 3.75 3.97 4.18 4.39 4.61&
4.82 5.04 5.25 5.47 5.68 5.89 6.11 6.32 6.54 6.75 6.96 7.18&
7.39 7.61 7.82 8.03 8.25 8.46 8.68 8.89 9.11 9.32 9.53 9.75&
9.96 10.18 10.39 10.6 10.82 11.03
SP1 D 0 0.0144 0.0334 0.0313 0.0281 0.025 0.0214 0.0198 0.0175&
0.0192 0.0222 0.0215 0.0225 0.0228 0.0295 0.0356 0.0368&
0.0346 0.0307 0.03 0.0269 0.0286 0.0318 0.0307 0.0333 0.0304&
0.0274 0.0233 0.0206 0.0181 0.0177 0.0204 0.0183 0.0163&
0.0168 0.0168 0.0188 0.0184 0.0169 0.0143 0.0097 0.0065&
0.0043 0.0037 0.0038 0.0051 0.0062 0.0055 0.0047 0.0037&
0.0028 0.0015 0.0004
SI2 = 0 0.1
F8:n,h,p 1
E8 0 1e-5 1e-3 1e-2 0.1 8i 1 89i 10
c material specification
M1 006012 -0.02 008016 -0.28 007014 -0.70 $air
M2 001001 -0.7273 006012 -0.2727 $propane c3h8
M3 001001 -0.102 006012 -0.768 008016 -0.0592 007014 -0.036 &
020040 -0.018 009019 -0.017 $A150

```

Section I.4 MCNPX simulation for the large detector with plastic shielding

```

Final program 1
c cell card
1 2 -0.000059 -1 -3 4 $large detector propane
2 3 -1.127 (1:3:-4) -2 -5 6 $large detector TEQC
3 2 -0.99 -9 10 -11 12 14 -13 $plastic board
4 1 -0.00191 -7 #1 #2 #3 $air
5 0 7 $outside area

c surface card
1 cx 0.5
2 cx 0.8
3 px 0.5
4 px -0.5
5 px 0.8
6 px -0.8
7 so 6
8 pz -3
9 px 0.8
10 px -0.8
11 py 0.8
12 py -0.8
13 pz -1
14 pz -2

mode n h p
IMP:n,h,p 1 1 1 0
nps 1e9
c source definition
SDEF par=1 erg=d1 POS=0 0 -3 VEC=0 0 1 DIR=1 SUR=8 RAD=d2 ext=0
SI1 H 4.14E-07 0.11 0.33 0.54 0.75 0.97 1.18 1.4 1.61 1.82 2.04&
2.25 2.47 2.68 2.9 3.11 3.32 3.54 3.75 3.97 4.18 4.39 4.61&
4.82 5.04 5.25 5.47 5.68 5.89 6.11 6.32 6.54 6.75 6.96 7.18&
7.39 7.61 7.82 8.03 8.25 8.46 8.68 8.89 9.11 9.32 9.53 9.75&
9.96 10.18 10.39 10.6 10.82 11.03
SP1 D 0 0.0144 0.0334 0.0313 0.0281 0.025 0.0214 0.0198 0.0175&
0.0192 0.0222 0.0215 0.0225 0.0228 0.0295 0.0356 0.0368&
0.0346 0.0307 0.03 0.0269 0.0286 0.0318 0.0307 0.0333 0.0304&
0.0274 0.0233 0.0206 0.0181 0.0177 0.0204 0.0183 0.0163&
0.0168 0.0168 0.0188 0.0184 0.0169 0.0143 0.0097 0.0065&
0.0043 0.0037 0.0038 0.0051 0.0062 0.0055 0.0047 0.0037&
0.0028 0.0015 0.0004
SI2 0 0.5
c SI3 = 1
F8:n,h,p 1
E8 0 1e-5 1e-2 0.1 8i 1 89i 10
c material specification
M1 006012 -0.02 008016 -0.28 007014 -0.70 $air
M2 001001 -0.7273 006012 -0.2727 $propane c3h8
M3 001001 -0.102 006012 -0.768 008016 -0.0592 007014 -0.036 &
020040 -0.018 009019 -0.017 $A150
print

```

Section I.5 MCNPX simulation for the small detector with plastic shielding

```

Final program 1
c cell card

```

```

1 2 -0.000059 -1 -3 4 $small detector air
2 3 -1.127 (1:3:-4) -2 -5 6 $small detector TEQC
3 2 -0.99 -9 10 -11 12 14 -13 $plastic board
4 1 -0.00191 -7 #1 #2 #3 $air
5 0 7 $outside area

c surface card
1 cx 0.1
2 cx 0.4
3 px 0.1
4 px -0.1
5 px 0.4
6 px -0.4
7 so 6
8 pz -3
9 px 0.8
10 px -0.8
11 py 0.8
12 py -0.8
13 pz -1
14 pz -2

mode n h p
IMP:n,h,p 1 1 1 1 0
nps 1e9

c source definition
SDEF par=1 erg=d1 POS=0 0 -3 VEC=0 0 1 DIR=1 RAD=d2 ext=0
SI1 H 4.14E-07 0.11 0.33 0.54 0.75 0.97 1.18 1.4 1.61 1.82 2.04&
2.25 2.47 2.68 2.9 3.11 3.32 3.54 3.75 3.97 4.18 4.39 4.61&
4.82 5.04 5.25 5.47 5.68 5.89 6.11 6.32 6.54 6.75 6.96 7.18&
7.39 7.61 7.82 8.03 8.25 8.46 8.68 8.89 9.11 9.32 9.53 9.75&
9.96 10.18 10.39 10.6 10.82 11.03
SP1 D 0 0.0144 0.0334 0.0313 0.0281 0.025 0.0214 0.0198 0.0175&
0.0192 0.0222 0.0215 0.0225 0.0228 0.0295 0.0356 0.0368&
0.0346 0.0307 0.03 0.0269 0.0286 0.0318 0.0307 0.0333 0.0304&
0.0274 0.0233 0.0206 0.0181 0.0177 0.0204 0.0183 0.0163&
0.0168 0.0168 0.0188 0.0184 0.0169 0.0143 0.0097 0.0065&
0.0043 0.0037 0.0038 0.0051 0.0062 0.0055 0.0047 0.0037&
0.0028 0.0015 0.0004
SI2 = 0 0.1
c SI3 = 1
F8:n,h,p 1
E8 0 1e-5 1e-3 1e-2 0.1 8i 1 89i 10
c material specification
M1 006012 -0.02 008016 -0.28 007014 -0.70 $air
M2 001001 -0.7273 006012 -0.2727 $propane c3h8
M3 001001 -0.102 006012 -0.768 008016 -0.0592 007014 -0.036 &
020040 -0.018 009019 -0.017 $A150
print
prdmp 2j 1

```

Section II Part of the MCNPX output

Section II.1 Part of the MCNPX output for the large detector without shielding

```
tally type 8      pulse height distribution.
cell 1
  energy
  0.0000E+00    1.00000E-09  1.0000
  1.0000E-05    9.67445E-01  0.0000
  1.0000E-03    5.67000E-07  0.0420
  1.0000E-02    2.46700E-06  0.0201
  1.0000E-01    1.00510E-05  0.0100
  2.0000E-01    5.91000E-06  0.0130
  3.0000E-01    4.12200E-06  0.0156
  4.0000E-01    3.14500E-06  0.0178
  5.0000E-01    2.61900E-06  0.0195
  6.0000E-01    2.20500E-06  0.0213
  7.0000E-01    1.86300E-06  0.0232
  8.0000E-01    1.66800E-06  0.0245
  9.0000E-01    1.53700E-06  0.0255
  1.0000E+00    1.39400E-06  0.0268
  1.1000E+00    1.31700E-06  0.0276
  1.2000E+00    1.23900E-06  0.0284
  1.3000E+00    1.19900E-06  0.0289
  1.4000E+00    1.02700E-06  0.0312
  1.5000E+00    1.01500E-06  0.0314
  1.6000E+00    9.57000E-07  0.0323
  1.7000E+00    9.12000E-07  0.0331
  1.8000E+00    8.76000E-07  0.0338
  1.9000E+00    8.09000E-07  0.0352
  2.0000E+00    7.88000E-07  0.0356
  2.1000E+00    8.28000E-07  0.0348
  2.2000E+00    7.40000E-07  0.0368
  2.3000E+00    7.00000E-07  0.0378
  2.4000E+00    6.66000E-07  0.0387
  2.5000E+00    6.88000E-07  0.0381
  2.6000E+00    6.18000E-07  0.0402
  2.7000E+00    6.11000E-07  0.0405
  2.8000E+00    6.18000E-07  0.0402
  2.9000E+00    5.56000E-07  0.0424
  3.0000E+00    5.10000E-07  0.0443
  3.1000E+00    5.04000E-07  0.0445
  3.2000E+00    4.43000E-07  0.0475
  3.3000E+00    4.28000E-07  0.0483
  3.4000E+00    4.01000E-07  0.0499
  3.5000E+00    3.92000E-07  0.0505
  3.6000E+00    3.88000E-07  0.0508
  3.7000E+00    3.65000E-07  0.0523
  3.8000E+00    3.13000E-07  0.0565
  3.9000E+00    3.19000E-07  0.0560
  4.0000E+00    3.06000E-07  0.0572
  4.1000E+00    2.72000E-07  0.0606
  4.2000E+00    2.81000E-07  0.0597
  4.3000E+00    2.61000E-07  0.0619
  4.4000E+00    2.48000E-07  0.0635
  4.5000E+00    2.35000E-07  0.0652
  4.6000E+00    2.08000E-07  0.0693
  4.7000E+00    2.37000E-07  0.0650
```

4.8000E+00	2.22000E-07	0.0671
4.9000E+00	1.89000E-07	0.0727
5.0000E+00	2.00000E-07	0.0707
5.1000E+00	1.67000E-07	0.0774
5.2000E+00	1.38000E-07	0.0851
5.3000E+00	1.26000E-07	0.0891
5.4000E+00	1.49000E-07	0.0819
5.5000E+00	1.15000E-07	0.0933
5.6000E+00	1.30000E-07	0.0877
5.7000E+00	1.24000E-07	0.0898
5.8000E+00	1.10000E-07	0.0953
5.9000E+00	8.80000E-08	0.1066
6.0000E+00	1.05000E-07	0.0976
6.1000E+00	9.80000E-08	0.1010
6.2000E+00	8.90000E-08	0.1060
6.3000E+00	7.20000E-08	0.1179
6.4000E+00	7.50000E-08	0.1155
6.5000E+00	7.80000E-08	0.1132
6.6000E+00	7.50000E-08	0.1155
6.7000E+00	5.40000E-08	0.1361
6.8000E+00	7.00000E-08	0.1195
6.9000E+00	5.50000E-08	0.1348
7.0000E+00	5.20000E-08	0.1387
7.1000E+00	5.10000E-08	0.1400
7.2000E+00	5.20000E-08	0.1387
7.3000E+00	4.60000E-08	0.1474
7.4000E+00	4.40000E-08	0.1508
7.5000E+00	3.70000E-08	0.1644
7.6000E+00	3.90000E-08	0.1601
7.7000E+00	3.50000E-08	0.1690
7.8000E+00	3.70000E-08	0.1644
7.9000E+00	2.90000E-08	0.1857
8.0000E+00	2.60000E-08	0.1961
8.1000E+00	2.40000E-08	0.2041
8.2000E+00	1.00000E-08	0.3162
8.3000E+00	1.30000E-08	0.2774
8.4000E+00	1.50000E-08	0.2582
8.5000E+00	1.70000E-08	0.2425
8.6000E+00	9.00000E-09	0.3333
8.7000E+00	9.00000E-09	0.3333
8.8000E+00	5.00000E-09	0.4472
8.9000E+00	9.00000E-09	0.3333
9.0000E+00	6.00000E-09	0.4082
9.1000E+00	9.00000E-09	0.3333
9.2000E+00	1.30000E-08	0.2774
9.3000E+00	8.00000E-09	0.3536
9.4000E+00	6.00000E-09	0.4082
9.5000E+00	3.00000E-09	0.5774
9.6000E+00	3.00000E-09	0.5774
9.7000E+00	8.00000E-09	0.3536
9.8000E+00	4.00000E-09	0.5000
9.9000E+00	3.00000E-09	0.5774
1.00000E+01	2.00000E-09	0.7071
total	9.67508E-01	0.0000

Section II.2 Part of the MCNPX output for the small detector without shielding

```
tally type 8      pulse height distribution.

cell 1
energy
0.0000E+00  0.00000E+00  0.0000
1.0000E-05  9.40732E-01  0.0000
1.0000E-03  8.30000E-08  0.1098
1.0000E-02  3.61000E-07  0.0526
1.0000E-01  1.71400E-06  0.0242
2.0000E-01  1.02400E-06  0.0312
3.0000E-01  7.36000E-07  0.0369
4.0000E-01  5.69000E-07  0.0419
5.0000E-01  4.89000E-07  0.0452
6.0000E-01  4.00000E-07  0.0500
7.0000E-01  3.27000E-07  0.0553
8.0000E-01  3.27000E-07  0.0553
9.0000E-01  3.04000E-07  0.0574
1.0000E+00  2.61000E-07  0.0619
1.1000E+00  2.48000E-07  0.0635
1.2000E+00  2.30000E-07  0.0659
1.3000E+00  2.50000E-07  0.0632
1.4000E+00  1.84000E-07  0.0737
1.5000E+00  2.19000E-07  0.0676
1.6000E+00  1.71000E-07  0.0765
1.7000E+00  1.56000E-07  0.0801
1.8000E+00  1.49000E-07  0.0819
1.9000E+00  1.49000E-07  0.0819
2.0000E+00  1.32000E-07  0.0870
2.1000E+00  1.56000E-07  0.0801
2.2000E+00  1.38000E-07  0.0851
2.3000E+00  1.32000E-07  0.0870
2.4000E+00  1.46000E-07  0.0828
2.5000E+00  1.23000E-07  0.0902
2.6000E+00  1.23000E-07  0.0902
2.7000E+00  1.10000E-07  0.0953
2.8000E+00  1.28000E-07  0.0884
2.9000E+00  9.10000E-08  0.1048
3.0000E+00  1.02000E-07  0.0990
3.1000E+00  8.40000E-08  0.1091
3.2000E+00  7.20000E-08  0.1179
3.3000E+00  7.50000E-08  0.1155
3.4000E+00  6.60000E-08  0.1231
3.5000E+00  6.20000E-08  0.1270
3.6000E+00  6.30000E-08  0.1260
3.7000E+00  7.20000E-08  0.1179
3.8000E+00  6.10000E-08  0.1280
3.9000E+00  6.00000E-08  0.1291
4.0000E+00  6.00000E-08  0.1291
4.1000E+00  3.50000E-08  0.1690
4.2000E+00  5.50000E-08  0.1348
4.3000E+00  4.50000E-08  0.1491
4.4000E+00  6.40000E-08  0.1250
4.5000E+00  3.70000E-08  0.1644
4.6000E+00  4.00000E-08  0.1581
4.7000E+00  4.30000E-08  0.1525
4.8000E+00  3.50000E-08  0.1690
4.9000E+00  3.80000E-08  0.1622
```

5.0000E+00	3.80000E-08	0.1622
5.1000E+00	2.50000E-08	0.2000
5.2000E+00	2.50000E-08	0.2000
5.3000E+00	2.20000E-08	0.2132
5.4000E+00	2.30000E-08	0.2085
5.5000E+00	1.90000E-08	0.2294
5.6000E+00	2.30000E-08	0.2085
5.7000E+00	2.40000E-08	0.2041
5.8000E+00	2.10000E-08	0.2182
5.9000E+00	2.00000E-08	0.2236
6.0000E+00	1.50000E-08	0.2582
6.1000E+00	1.50000E-08	0.2582
6.2000E+00	2.00000E-08	0.2236
6.3000E+00	1.30000E-08	0.2774
6.4000E+00	1.00000E-08	0.3162
6.5000E+00	1.30000E-08	0.2774
6.6000E+00	1.90000E-08	0.2294
6.7000E+00	9.00000E-09	0.3333
6.8000E+00	1.90000E-08	0.2294
6.9000E+00	6.00000E-09	0.4082
7.0000E+00	1.00000E-08	0.3162
7.1000E+00	1.30000E-08	0.2774
7.2000E+00	1.40000E-08	0.2673
7.3000E+00	6.00000E-09	0.4082
7.4000E+00	9.00000E-09	0.3333
7.5000E+00	6.00000E-09	0.4082
7.6000E+00	4.00000E-09	0.5000
7.7000E+00	8.00000E-09	0.3536
7.8000E+00	4.00000E-09	0.5000
7.9000E+00	6.00000E-09	0.4082
8.0000E+00	1.00000E-08	0.3162
8.1000E+00	8.00000E-09	0.3536
8.2000E+00	2.00000E-09	0.7071
8.3000E+00	5.00000E-09	0.4472
8.4000E+00	6.00000E-09	0.4082
8.5000E+00	7.00000E-09	0.3780
8.6000E+00	1.00000E-09	1.0000
8.7000E+00	3.00000E-09	0.5774
8.8000E+00	1.00000E-09	1.0000
8.9000E+00	1.00000E-09	1.0000
9.0000E+00	0.00000E+00	0.0000
9.1000E+00	1.00000E-09	1.0000
9.2000E+00	8.00000E-09	0.3536
9.3000E+00	1.00000E-09	1.0000
9.4000E+00	2.00000E-09	0.7071
9.5000E+00	2.00000E-09	0.7071
9.6000E+00	1.00000E-09	1.0000
9.7000E+00	2.00000E-09	0.7071
9.8000E+00	0.00000E+00	0.0000
9.9000E+00	0.00000E+00	0.0000
1.0000E+01	0.00000E+00	0.0000
total	9.40744E-01	0.0000

Section II.3 Part of the MCNPX output for the large detector with plastic shielding

tally type 8 pulse height distribution.

```

cell 1
energy
0.0000E+00 1.09000E-06 0.0303
1.0000E-05 4.71375E-01 0.0000
1.0000E-03 1.80400E-06 0.0235
1.0000E-02 1.36600E-06 0.0271
1.0000E-01 2.34300E-06 0.0207
2.0000E-01 1.16700E-06 0.0293
3.0000E-01 9.98000E-07 0.0317
4.0000E-01 8.32000E-07 0.0347
5.0000E-01 7.34000E-07 0.0369
6.0000E-01 6.02000E-07 0.0408
7.0000E-01 6.21000E-07 0.0401
8.0000E-01 5.98000E-07 0.0409
9.0000E-01 5.33000E-07 0.0433
1.0000E+00 5.21000E-07 0.0438
1.1000E+00 4.61000E-07 0.0466
1.2000E+00 4.61000E-07 0.0466
1.3000E+00 4.44000E-07 0.0475
1.4000E+00 4.28000E-07 0.0483
1.5000E+00 4.48000E-07 0.0472
1.6000E+00 3.82000E-07 0.0512
1.7000E+00 4.07000E-07 0.0496
1.8000E+00 3.52000E-07 0.0533
1.9000E+00 3.67000E-07 0.0522
2.0000E+00 3.55000E-07 0.0531
2.1000E+00 2.91000E-07 0.0586
2.2000E+00 3.32000E-07 0.0549
2.3000E+00 2.96000E-07 0.0581
2.4000E+00 2.80000E-07 0.0598
2.5000E+00 2.83000E-07 0.0594
2.6000E+00 2.77000E-07 0.0601
2.7000E+00 2.73000E-07 0.0605
2.8000E+00 2.62000E-07 0.0618
2.9000E+00 2.62000E-07 0.0618
3.0000E+00 2.16000E-07 0.0680
3.1000E+00 2.37000E-07 0.0650
3.2000E+00 2.09000E-07 0.0692
3.3000E+00 2.12000E-07 0.0687
3.4000E+00 2.32000E-07 0.0657
3.5000E+00 1.85000E-07 0.0735
3.6000E+00 1.95000E-07 0.0716
3.7000E+00 1.86000E-07 0.0733
3.8000E+00 1.79000E-07 0.0747
3.9000E+00 1.49000E-07 0.0819
4.0000E+00 1.42000E-07 0.0839
4.1000E+00 1.22000E-07 0.0905
4.2000E+00 1.59000E-07 0.0793
4.3000E+00 1.24000E-07 0.0898
4.4000E+00 1.27000E-07 0.0887
4.5000E+00 1.06000E-07 0.0971
4.6000E+00 1.25000E-07 0.0894
4.7000E+00 1.35000E-07 0.0861
4.8000E+00 1.16000E-07 0.0928
4.9000E+00 1.11000E-07 0.0949
5.0000E+00 9.50000E-08 0.1026
5.1000E+00 8.90000E-08 0.1060
5.2000E+00 9.90000E-08 0.1005
5.3000E+00 6.70000E-08 0.1222

```

5.4000E+00	7.90000E-08	0.1125
5.5000E+00	6.80000E-08	0.1213
5.6000E+00	7.00000E-08	0.1195
5.7000E+00	5.40000E-08	0.1361
5.8000E+00	5.60000E-08	0.1336
5.9000E+00	5.40000E-08	0.1361
6.0000E+00	4.50000E-08	0.1491
6.1000E+00	4.50000E-08	0.1491
6.2000E+00	5.60000E-08	0.1336
6.3000E+00	6.00000E-08	0.1291
6.4000E+00	5.10000E-08	0.1400
6.5000E+00	3.40000E-08	0.1715
6.6000E+00	2.80000E-08	0.1890
6.7000E+00	4.00000E-08	0.1581
6.8000E+00	4.10000E-08	0.1562
6.9000E+00	3.30000E-08	0.1741
7.0000E+00	3.30000E-08	0.1741
7.1000E+00	2.10000E-08	0.2182
7.2000E+00	2.70000E-08	0.1925
7.3000E+00	3.00000E-08	0.1826
7.4000E+00	2.20000E-08	0.2132
7.5000E+00	1.90000E-08	0.2294
7.6000E+00	1.50000E-08	0.2582
7.7000E+00	2.10000E-08	0.2182
7.8000E+00	1.30000E-08	0.2774
7.9000E+00	2.00000E-08	0.2236
8.0000E+00	1.50000E-08	0.2582
8.1000E+00	1.10000E-08	0.3015
8.2000E+00	5.00000E-09	0.4472
8.3000E+00	6.00000E-09	0.4082
8.4000E+00	5.00000E-09	0.4472
8.5000E+00	5.00000E-09	0.4472
8.6000E+00	6.00000E-09	0.4082
8.7000E+00	4.00000E-09	0.5000
8.8000E+00	5.00000E-09	0.4472
8.9000E+00	9.00000E-09	0.3333
9.0000E+00	1.00000E-09	1.0000
9.1000E+00	5.00000E-09	0.4472
9.2000E+00	5.00000E-09	0.4472
9.3000E+00	8.00000E-09	0.3536
9.4000E+00	4.00000E-09	0.5000
9.5000E+00	4.00000E-09	0.5000
9.6000E+00	6.00000E-09	0.4082
9.7000E+00	4.00000E-09	0.5000
9.8000E+00	0.00000E+00	0.0000
9.9000E+00	0.00000E+00	0.0000
1.0000E+01	4.00000E-09	0.5000
total	4.71400E-01	0.0000

Section II.4 Part of the MCNPX output for the small detector with plastic shielding

```
tally type 8      pulse height distribution.

cell 1
  energy
 0.0000E+00    7.00000E-09  0.3780
```

1.0000E-05	3.81708E-01	0.0000
1.0000E-03	2.20000E-08	0.2132
1.0000E-02	4.40000E-08	0.1508
1.0000E-01	1.33000E-07	0.0867
2.0000E-01	1.24000E-07	0.0898
3.0000E-01	1.54000E-07	0.0806
4.0000E-01	8.90000E-08	0.1060
5.0000E-01	1.14000E-07	0.0937
6.0000E-01	1.09000E-07	0.0958
7.0000E-01	1.02000E-07	0.0990
8.0000E-01	9.90000E-08	0.1005
9.0000E-01	9.90000E-08	0.1005
1.0000E+00	7.10000E-08	0.1187
1.1000E+00	9.50000E-08	0.1026
1.2000E+00	6.30000E-08	0.1260
1.3000E+00	9.10000E-08	0.1048
1.4000E+00	6.50000E-08	0.1240
1.5000E+00	6.70000E-08	0.1222
1.6000E+00	7.50000E-08	0.1155
1.7000E+00	6.80000E-08	0.1213
1.8000E+00	6.30000E-08	0.1260
1.9000E+00	6.70000E-08	0.1222
2.0000E+00	6.40000E-08	0.1250
2.1000E+00	6.20000E-08	0.1270
2.2000E+00	5.30000E-08	0.1374
2.3000E+00	6.80000E-08	0.1213
2.4000E+00	6.00000E-08	0.1291
2.5000E+00	5.50000E-08	0.1348
2.6000E+00	3.90000E-08	0.1601
2.7000E+00	3.60000E-08	0.1667
2.8000E+00	5.50000E-08	0.1348
2.9000E+00	5.70000E-08	0.1325
3.0000E+00	5.00000E-08	0.1414
3.1000E+00	4.60000E-08	0.1474
3.2000E+00	4.10000E-08	0.1562
3.3000E+00	4.30000E-08	0.1525
3.4000E+00	3.60000E-08	0.1667
3.5000E+00	3.90000E-08	0.1601
3.6000E+00	3.20000E-08	0.1768
3.7000E+00	3.40000E-08	0.1715
3.8000E+00	3.90000E-08	0.1601
3.9000E+00	3.50000E-08	0.1690
4.0000E+00	2.90000E-08	0.1857
4.1000E+00	2.10000E-08	0.2182
4.2000E+00	2.30000E-08	0.2085
4.3000E+00	2.60000E-08	0.1961
4.4000E+00	2.20000E-08	0.2132
4.5000E+00	1.70000E-08	0.2425
4.6000E+00	2.10000E-08	0.2182
4.7000E+00	1.80000E-08	0.2357
4.8000E+00	1.20000E-08	0.2887
4.9000E+00	1.50000E-08	0.2582
5.0000E+00	1.20000E-08	0.2887
5.1000E+00	1.90000E-08	0.2294
5.2000E+00	2.20000E-08	0.2132
5.3000E+00	1.60000E-08	0.2500
5.4000E+00	1.50000E-08	0.2582
5.5000E+00	8.00000E-09	0.3536
5.6000E+00	1.00000E-08	0.3162
5.7000E+00	1.50000E-08	0.2582

5.8000E+00	1.10000E-08	0.3015
5.9000E+00	1.10000E-08	0.3015
6.0000E+00	1.20000E-08	0.2887
6.1000E+00	1.00000E-08	0.3162
6.2000E+00	1.20000E-08	0.2887
6.3000E+00	8.00000E-09	0.3536
6.4000E+00	7.00000E-09	0.3780
6.5000E+00	1.20000E-08	0.2887
6.6000E+00	9.00000E-09	0.3333
6.7000E+00	9.00000E-09	0.3333
6.8000E+00	9.00000E-09	0.3333
6.9000E+00	1.40000E-08	0.2673
7.0000E+00	7.00000E-09	0.3780
7.1000E+00	6.00000E-09	0.4082
7.2000E+00	6.00000E-09	0.4082
7.3000E+00	6.00000E-09	0.4082
7.4000E+00	3.00000E-09	0.5774
7.5000E+00	8.00000E-09	0.3536
7.6000E+00	3.00000E-09	0.5774
7.7000E+00	4.00000E-09	0.5000
7.8000E+00	2.00000E-09	0.7071
7.9000E+00	4.00000E-09	0.5000
8.0000E+00	5.00000E-09	0.4472
8.1000E+00	1.00000E-09	1.0000
8.2000E+00	1.00000E-09	1.0000
8.3000E+00	2.00000E-09	0.7071
8.4000E+00	1.00000E-09	1.0000
8.5000E+00	2.00000E-09	0.7071
8.6000E+00	1.00000E-09	1.0000
8.7000E+00	0.00000E+00	0.0000
8.8000E+00	0.00000E+00	0.0000
8.9000E+00	2.00000E-09	0.7071
9.0000E+00	0.00000E+00	0.0000
9.1000E+00	1.00000E-09	1.0000
9.2000E+00	1.00000E-09	1.0000
9.3000E+00	0.00000E+00	0.0000
9.4000E+00	1.00000E-09	1.0000
9.5000E+00	0.00000E+00	0.0000
9.6000E+00	1.00000E-09	1.0000
9.7000E+00	0.00000E+00	0.0000
9.8000E+00	2.00000E-09	0.7071
9.9000E+00	0.00000E+00	0.0000
1.00000E+01	1.00000E-09	1.0000
total	3.81711E-01	0.0000

APPENDIX B
ORIGINAL DATA

Section I: Data set 1 for ^{241}Am - ^9Be neutron source without Shielding-4hrs

Large Detector, High Gain

***** S P E C T R A L D A T A R E P O R T *****

***** Sample ID: *****

Elapsed Live time: 12090
Elapsed Real Time: 14400

Channel	-----	-----	-----	-----	-----	-----	-----	-----
1:	0	0	0	0	0	0	0	0
9:	15	2	0	0	0	0	574	3751
17:	7713848	8802874	6557979	4842653	3565542	2618313	1917106	1403196
25:	1032603	763258	566577	427832	324925	253892	199742	160320
33:	131071	109572	93908	80790	71714	64349	57621	52838
41:	49067	45381	42119	39677	37789	35763	33745	32637
49:	30912	30093	28633	27580	26867	25523	25006	24128
57:	23208	22663	21959	21286	20905	20258	19622	19120
65:	18537	17995	17498	17181	16915	16375	15904	15530
73:	15143	14758	14441	14108	13791	13391	13231	12817
81:	12950	12128	12199	11972	11725	11372	11392	11178
89:	10871	10631	10509	10420	10232	9914	9861	9556
97:	9693	9304	9345	9259	8947	8690	8775	8748
105:	8594	8455	8217	8060	8105	7927	8026	7787
113:	7638	7540	7426	7328	7160	7163	7138	7029
121:	6951	6912	6549	6811	6570	6673	6383	6315
129:	6268	6131	6221	6222	5898	6026	5847	5859
137:	5731	5801	5613	5605	5512	5565	5535	5510
145:	5286	5265	5206	5189	5068	4999	5008	5128
153:	4838	4787	4683	4750	4696	4662	4639	4638
161:	4480	4458	4593	4453	4470	4374	4290	4215
169:	4274	4176	4016	4104	4149	4067	4065	3883
177:	3908	3903	3848	3834	3912	3743	3670	3724
185:	3669	3535	3582	3595	3499	3526	3480	3408
193:	3408	3413	3333	3402	3334	3191	3197	3190
201:	3167	3192	3174	3012	3026	3009	3070	2979
209:	2861	2857	2881	2952	2808	2815	2789	2819
217:	2783	2700	2718	2610	2671	2559	2608	2601
225:	2606	2525	2420	2453	2509	2489	2421	2371
233:	2288	2376	2286	2199	2208	2186	2200	2155

241:	2082	2135	2061	2109	2101	2042	2041	2021
249:	2073	2020	1966	2010	1917	1849	1874	1838
257:	1748	1835	1735	1776	1722	1784	1746	1716
265:	1696	1628	1628	1712	1605	1579	1551	1573
273:	1555	1585	1545	1553	1526	1513	1400	1503
281:	1428	1369	1421	1348	1286	1349	1286	1321
289:	1273	1237	1214	1215	1268	1166	1227	1204
297:	1188	1171	1227	1162	1150	1102	1146	1081
305:	1107	1064	1168	1041	1102	1010	1081	1111
313:	1026	964	985	965	938	942	1019	977
321:	909	905	945	957	914	892	877	896
329:	848	828	870	817	854	832	814	813
337:	793	791	792	803	757	767	742	742
345:	781	772	769	784	742	768	733	722
353:	726	743	717	771	739	670	725	671
361:	660	726	645	731	688	692	691	636
369:	625	672	643	623	706	600	638	640
377:	610	628	618	639	603	611	571	578
385:	636	652	583	622	666	571	595	567
393:	599	597	544	573	556	566	542	571
401:	567	623	558	539	573	572	555	546
409:	579	570	582	526	552	514	583	546
417:	507	536	507	548	490	515	548	535
425:	535	524	521	518	588	508	521	494
433:	515	515	525	497	499	562	482	538
441:	535	535	499	501	489	493	498	463
449:	480	476	488	533	485	488	521	520
457:	495	458	496	466	468	477	477	479
465:	513	484	468	462	495	488	489	481
473:	476	481	485	470	470	463	465	462
481:	490	474	482	456	452	460	463	418
489:	447	462	465	455	467	448	419	458
497:	450	466	437	472	462	427	400	460
505:	407	454	431	393	451	412	428	434
513:	466	460	438	432	450	427	428	421
521:	434	436	450	422	442	448	393	423
529:	437	438	425	430	435	420	426	379
537:	409	425	392	417	419	398	421	427
545:	405	412	390	429	377	383	443	433
553:	422	391	422	389	378	408	406	372
561:	414	405	418	373	403	384	402	341
569:	373	374	430	390	395	372	372	386
577:	375	385	378	396	382	399	365	410
585:	397	384	397	378	383	380	404	401
593:	348	370	375	368	374	386	370	405
601:	358	355	396	348	386	368	388	365
609:	369	339	364	364	358	380	364	355
617:	329	336	335	362	372	337	368	387
625:	376	330	379	362	372	371	371	362
633:	326	354	372	344	324	338	332	320
641:	344	373	348	367	328	318	340	344
649:	343	360	366	333	340	337	349	366
657:	317	345	350	323	319	300	279	369
665:	338	333	309	325	353	315	326	334

673:	329	342	368	301	302	316	353	278
681:	315	311	332	325	309	342	355	287
689:	344	280	299	303	325	303	316	299
697:	344	301	317	314	309	305	320	298
705:	324	330	275	302	319	331	290	285
713:	287	306	267	326	308	293	290	300
721:	281	311	303	259	306	301	291	295
729:	279	258	269	331	275	283	293	271
737:	319	280	265	286	320	307	277	288
745:	260	273	311	278	248	267	292	280
753:	261	272	308	286	248	294	286	276
761:	267	275	262	287	277	283	296	286
769:	293	259	268	273	271	277	246	263
777:	257	270	288	267	240	256	280	255
785:	276	264	277	236	285	261	256	256
793:	274	261	253	280	259	255	241	239

Large Detector, Low Gain

 ***** S P E C T R A L D A T A R E P O R T *****

***** Sample ID: *****

Elapsed Live time: 14394
 Elapsed Real Time: 14400

Channel	-----	-----	-----	-----	-----	-----	-----	-----
1:	0	0	0	0	0	0	0	0
9:	0	0	0	0	0	0	0	405
17:	13085	12443	11908	11181	10872	10260	9858	9411
25:	9055	8777	8320	7895	7619	7141	6983	6662
33:	6277	6012	5712	5355	5141	4953	4644	4524
41:	4333	4111	3978	3674	3527	3305	3214	3135
49:	2950	2811	2664	2528	2503	2306	2269	2176
57:	2116	1971	1845	1798	1681	1718	1669	1580
65:	1571	1418	1420	1352	1344	1208	1223	1168
73:	1112	1064	1059	1060	973	950	941	920
81:	860	801	775	777	743	815	729	743
89:	695	679	664	649	629	595	602	552
97:	557	514	513	559	504	491	481	476
105:	460	454	415	414	387	422	411	358
113:	332	352	333	334	370	343	334	295
121:	301	298	268	287	299	263	259	226
129:	274	240	264	267	267	265	260	211
137:	209	217	226	216	222	230	180	198
145:	235	185	202	198	191	190	177	170
153:	167	190	149	176	174	170	146	150
161:	136	150	140	152	155	147	159	128
169:	127	137	129	119	165	114	127	136
177:	121	121	131	122	115	117	124	115

185:	90	115	90	103	92	92	95	87
193:	92	101	82	89	89	84	87	84
201:	76	80	81	63	86	97	60	76
209:	47	61	60	58	66	60	63	55
217:	56	51	44	48	55	54	50	31
225:	45	38	34	44	32	36	21	29
233:	20	33	37	37	29	23	33	24
241:	27	23	17	23	13	16	16	21
249:	19	16	16	20	17	10	19	10
257:	16	21	10	11	12	9	10	9
265:	11	17	9	14	16	18	14	8
273:	10	10	8	4	5	9	10	7
281:	6	7	6	11	8	11	8	8
289:	4	7	9	5	7	5	7	8
297:	11	7	10	10	14	8	9	6
305:	4	14	5	3	6	13	10	5
313:	4	11	4	10	6	2	11	4
321:	4	4	5	6	8	6	8	4
329:	5	7	5	6	7	6	4	6
337:	5	7	5	8	6	8	4	4
345:	7	6	4	4	4	9	7	6
353:	8	8	7	3	5	7	4	2
361:	5	7	9	9	4	4	6	6
369:	5	7	8	4	11	7	6	6
377:	2	4	6	2	8	6	3	3
385:	4	3	6	2	4	2	10	10
393:	3	8	5	6	4	6	3	1
401:	5	2	3	4	3	5	7	7
409:	6	2	3	2	1	7	7	4
417:	7	4	5	0	4	4	4	3
425:	2	2	4	4	5	2	6	4
433:	2	3	6	7	3	6	5	4
441:	6	1	5	3	4	6	6	3
449:	3	7	5	4	4	6	0	4
457:	6	3	5	8	4	4	6	3
465:	5	2	4	5	1	6	4	5
473:	3	1	8	3	4	3	3	2
481:	8	1	0	7	4	7	4	6
489:	8	4	4	0	6	2	4	6
497:	7	5	3	4	3	3	5	0
505:	3	1	4	5	3	2	2	3
513:	0	3	5	3	4	0	0	5
521:	4	5	4	3	4	3	2	2
529:	4	2	2	3	3	2	4	4
537:	1	2	1	3	3	4	1	1
545:	4	2	1	4	2	2	4	3
553:	2	6	1	2	3	5	2	4
561:	3	3	5	1	4	2	4	1
569:	5	3	4	4	3	2	2	3
577:	4	6	3	3	2	5	4	3
585:	5	3	2	0	2	5	1	2
593:	3	3	2	4	6	2	2	3
601:	4	5	4	1	1	2	1	2
609:	1	3	2	3	1	3	5	2

617:	5	3	2	2	0	3	3	2
625:	4	0	2	3	1	3	1	2
633:	3	1	2	3	2	4	1	0
641:	5	1	2	0	2	2	3	3
649:	5	2	3	0	5	3	2	2
657:	1	1	1	3	5	2	1	1
665:	2	1	0	2	4	4	1	1
673:	0	2	3	3	3	2	2	3
681:	1	2	0	1	1	0	1	2
689:	1	1	1	1	1	1	3	3
697:	2	1	1	1	3	2	3	2
705:	3	0	2	3	1	0	3	1
713:	1	2	1	3	1	1	1	1
721:	2	0	2	1	3	5	1	0
729:	4	1	0	2	1	1	1	0
737:	1	1	2	2	1	4	1	2
745:	1	1	1	2	1	0	2	1
753:	2	1	2	2	0	0	2	1
761:	1	1	4	2	0	2	1	1
769:	3	0	0	1	2	1	0	2
777:	2	0	1	0	1	0	3	1
785:	2	0	1	1	1	0	2	1
793:	2	0	0	2	0	0	1	1

Small Detector, High Gain

***** S P E C T R A L D A T A R E P O R T *****

***** Sample ID: *****

Elapsed Live time: 12886
 Elapsed Real Time: 14400

Channel	-----	-----	-----	-----	-----	-----	-----	-----
1:	0	0	0	0	0	0	0	0
9:	0	0	0	0	0	3	8264	189562
17:	3531877	2985029	2149289	1510012	1036599	694629	454206	293516
25:	187572	120001	76628	51426	35098	25553	19573	15934
33:	13460	11789	10656	9657	8967	8491	7929	7425
41:	7151	6586	6359	6016	5777	5377	5097	4936
49:	4745	4460	4287	3980	4040	3760	3704	3534
57:	3455	3443	3293	3234	3083	3106	2947	2882
65:	2890	2670	2646	2510	2442	2340	2328	2325
73:	2280	2145	2139	2084	2044	1953	2017	1923
81:	1928	1795	1801	1823	1738	1782	1639	1676
89:	1604	1613	1636	1539	1525	1523	1564	1469
97:	1458	1386	1313	1395	1319	1343	1241	1291
105:	1250	1244	1275	1248	1197	1217	1158	1174
113:	1118	1144	1058	1117	1054	1061	1021	1060
121:	1005	988	1006	1025	1011	949	972	934
129:	920	926	923	931	887	952	876	911

137:	853	879	852	864	804	792	854	803
145:	791	857	786	784	807	748	736	771
153:	759	723	731	707	710	700	714	689
161:	683	663	672	678	661	678	670	664
169:	633	608	627	651	621	597	581	627
177:	578	539	615	579	597	534	557	634
185:	571	602	554	541	575	495	541	549
193:	506	532	523	483	506	543	506	511
201:	479	479	506	464	458	451	430	423
209:	465	467	435	436	419	421	436	406
217:	423	448	414	430	425	480	389	386
225:	396	415	385	375	376	363	337	380
233:	337	353	352	362	337	352	346	358
241:	342	320	309	337	288	339	318	317
249:	360	335	348	317	333	304	300	270
257:	286	294	291	300	276	294	273	300
265:	291	248	286	320	269	250	241	249
273:	254	273	295	253	287	257	260	248
281:	227	251	264	224	259	213	243	238
289:	267	226	210	233	214	231	254	218
297:	226	210	204	234	208	215	187	221
305:	210	214	224	190	212	200	214	193
313:	199	193	186	216	192	186	169	217
321:	192	180	193	210	178	199	162	177
329:	173	176	177	199	156	178	178	151
337:	153	184	159	159	151	160	172	144
345:	180	172	161	169	163	154	137	137
353:	143	151	165	152	152	146	159	154
361:	138	165	165	137	147	140	131	142
369:	132	138	137	151	135	141	151	149
377:	151	119	140	134	130	140	113	140
385:	143	129	151	126	136	127	131	119
393:	114	131	127	111	115	111	124	138
401:	128	126	111	127	105	129	114	100
409:	118	116	108	129	117	105	127	130
417:	119	110	108	119	103	120	120	122
425:	100	101	121	109	109	122	103	101
433:	92	96	125	111	99	112	99	102
441:	108	98	112	95	113	102	101	116
449:	99	122	99	107	101	90	94	83
457:	116	86	74	105	92	84	77	103
465:	85	89	96	107	113	87	80	88
473:	101	83	88	80	100	107	103	81
481:	95	112	95	72	81	93	89	78
489:	89	74	91	88	80	95	80	87
497:	88	72	80	84	65	76	92	67
505:	64	79	82	63	73	57	79	70
513:	81	76	78	80	75	80	72	66
521:	79	65	75	79	78	69	73	66
529:	60	70	69	72	81	73	80	73
537:	86	71	67	70	60	58	63	73
545:	69	59	67	59	70	59	65	61
553:	60	57	75	65	63	59	70	62
561:	65	57	48	73	63	74	78	57

569:	57	66	59	76	62	57	57	66
577:	60	64	59	64	50	56	50	59
585:	71	60	71	50	54	47	50	69
593:	70	53	53	53	51	49	62	58
601:	49	49	58	54	67	53	65	58
609:	60	58	46	50	49	55	57	59
617:	48	40	60	64	56	45	56	53
625:	49	60	52	48	63	50	52	52
633:	60	53	54	42	47	47	43	46
641:	55	42	40	35	49	40	33	47
649:	50	41	61	41	58	40	45	47
657:	51	44	48	50	37	51	37	46
665:	42	40	40	41	41	36	46	34
673:	44	44	46	39	41	40	37	43
681:	28	37	40	62	31	48	47	27
689:	45	32	40	34	33	43	35	38
697:	43	29	40	43	41	48	39	38
705:	47	42	35	33	32	37	35	44
713:	31	42	45	45	29	31	32	40
721:	28	35	27	36	32	31	31	30
729:	23	39	27	36	33	35	35	35
737:	28	32	40	34	32	35	26	34
745:	25	41	40	24	37	29	44	43
753:	40	32	37	35	24	43	24	35
761:	30	38	44	41	33	28	40	29
769:	27	28	33	36	34	24	27	31
777:	34	26	30	29	20	27	29	40
785:	22	31	26	34	29	29	24	34
793:	21	32	26	32	26	28	30	37

Small Detector, Low Gain

***** S P E C T R A L D A T A R E P O R T *****

***** Sample ID: *****

Elapsed Live time: 14206

Elapsed Real Time: 14400

Channel	-----	-----	-----	-----	-----	-----	-----	-----
1:	235	3321	8094	9318	8631	7824	7152	6278
9:	5623	5036	4388	3962	3456	3150	2878	2600
17:	2412	2207	1997	1838	1644	1480	1432	1330
25:	1230	1111	977	917	847	751	792	679
33:	587	595	505	570	475	467	461	418
41:	366	392	346	314	289	239	279	253
49:	260	227	210	215	215	171	160	153
57:	154	149	159	153	123	140	117	116
65:	121	125	122	114	106	101	79	90
73:	79	84	80	86	83	75	73	84
81:	65	77	64	72	62	51	77	62
89:	60	56	38	51	63	47	57	40
97:	53	43	32	29	30	39	31	34
105:	36	22	28	31	29	25	16	18

113:	14	24	17	17	18	22	15	19
121:	17	8	12	11	12	10	14	13
129:	17	8	12	7	13	7	7	6
137:	12	6	7	8	6	7	4	8
145:	5	7	7	2	8	8	5	6
153:	6	8	6	3	5	2	6	3
161:	2	2	7	4	4	4	4	2
169:	12	4	2	4	4	6	4	3
177:	3	7	3	2	2	3	2	3
185:	5	1	2	3	4	1	1	3
193:	6	2	0	1	1	0	6	2
201:	1	2	1	4	6	1	4	3
209:	1	4	4	3	3	4	1	3
217:	2	3	2	0	2	3	5	2
225:	0	1	5	0	3	2	3	5
233:	1	0	4	1	2	2	2	0
241:	2	2	0	3	0	1	1	1
249:	1	1	2	6	3	2	1	5
257:	1	4	2	1	0	2	2	1
265:	0	0	3	0	3	0	2	1
273:	0	2	2	1	2	0	1	3
281:	1	3	0	1	1	0	2	3
289:	1	1	2	3	1	0	2	1
297:	1	1	3	1	2	1	1	1
305:	1	0	0	2	0	0	0	0
313:	1	1	2	3	1	1	2	1
321:	1	3	0	1	1	2	0	0
329:	1	2	0	0	2	2	0	2
337:	0	1	0	1	0	0	1	3
345:	1	3	0	0	2	0	1	0
353:	1	1	1	1	0	0	1	0
361:	0	0	1	1	1	1	0	2
377:	0	1	0	0	0	0	0	1
385:	1	0	0	0	2	2	2	4
393:	0	1	0	1	0	1	0	1
401:	2	1	2	0	0	1	0	0
409:	1	1	0	0	0	1	0	1
417:	0	0	0	0	2	1	0	0
425:	0	0	1	0	0	1	0	0
433:	1	0	0	0	2	0	0	0
441:	0	0	2	1	1	1	0	0
449:	0	0	0	3	1	2	0	0
457:	1	1	1	1	1	1	1	0
465:	0	1	1	1	0	0	0	0
473:	1	1	0	0	0	0	2	1
481:	0	0	0	0	0	1	0	0
489:	0	0	2	1	0	0	1	1
497:	0	0	0	0	0	1	0	0
505:	0	0	0	1	0	0	1	0
513:	1	0	0	0	0	0	1	0
521:	0	0	1	0	1	0	1	0
529:	0	0	0	0	0	0	0	2
537:	0	1	0	1	0	0	1	0
545:	0	0	0	1	0	0	1	0

553:	0	0	0	0	0	1	0	0
561:	0	1	0	0	0	0	0	0
569:	0	0	0	0	1	0	1	0
577:	0	0	0	1	0	0	0	0
585:	0	0	0	0	0	0	0	0
593:	0	0	1	0	0	0	0	0
601:	0	0	0	0	0	0	0	0
609:	0	0	0	0	0	0	0	1
617:	0	0	0	0	0	0	1	0
625:	0	0	0	0	0	0	0	0
633:	0	0	0	0	1	0	0	0
641:	0	1	0	0	0	0	0	0
649:	0	0	0	1	1	0	0	0
657:	0	0	0	0	1	0	0	0
665:	0	0	1	0	0	0	0	0
673:	0	1	0	0	0	1	1	0
681:	0	0	0	0	0	1	0	0
689:	1	0	0	0	1	0	0	0
697:	0	0	0	0	0	0	0	0
705:	0	0	0	0	0	0	1	0
713:	0	0	0	0	0	0	0	0
721:	0	0	0	0	0	0	0	0
729:	0	0	0	0	0	0	0	0
737:	0	0	0	0	0	0	0	0
745:	0	0	0	0	0	0	0	0
753:	0	0	0	0	0	0	0	0
761:	0	0	0	0	0	0	0	0
769:	0	0	0	0	0	0	0	0
777:	0	0	0	0	0	0	0	0
785:	0	0	0	0	1	0	0	0
793:	1	0	0	0	0	0	0	0

Section II: Data set 2 for background-4hrs

Large Detector, High Gain

```
*****
*****      S P E C T R A L      D A T A      R E P O R T      *****
*****
```

***** Sample ID: *****

Elapsed Live time: 11346
Elapsed Real Time: 14400

Channel	-----	-----	-----	-----	-----	-----	-----	-----
1:	0	0	0	0	0	0	0	0
9:	0	0	0	0	0	0	922	6127
17:	*****	*****	*****	9580117	7505775	5840731	4510181	3458167

457:	1	0	0	0	0	1	1	0
465:	1	0	0	0	0	0	0	0
473:	0	0	0	0	1	1	0	0
481:	0	1	0	0	0	0	0	1
489:	0	0	0	1	0	0	0	1
497:	0	0	1	0	0	0	1	0
505:	0	0	0	1	0	0	0	0
513:	0	2	0	0	0	0	0	0
521:	0	0	0	0	0	0	1	0
529:	0	0	0	0	0	0	0	0
537:	0	0	0	0	0	0	0	0
545:	0	0	1	0	0	0	0	0
553:	0	0	0	0	0	0	0	0
561:	0	0	0	0	0	0	1	2
569:	0	0	1	0	0	0	2	0
577:	0	0	0	0	0	0	0	0
585:	0	0	0	0	0	0	0	1
593:	0	0	0	0	0	0	0	0
601:	0	0	1	0	0	0	0	0
609:	0	0	0	0	0	0	0	0
617:	0	0	0	0	0	0	0	0
625:	0	0	0	0	0	0	0	0
633:	0	0	0	1	0	0	0	0
641:	0	0	1	0	0	0	0	0
649:	0	0	0	0	0	0	0	0
657:	0	0	0	0	1	0	0	0
665:	0	0	1	0	0	0	0	0
673:	0	0	0	0	1	0	0	0
681:	0	0	0	0	0	0	1	0
689:	0	0	0	0	0	0	0	0
697:	0	0	0	0	0	0	0	0
705:	0	0	0	0	0	0	0	0
713:	0	0	0	0	0	0	0	0
721:	0	0	0	0	0	0	0	0
729:	0	0	0	0	0	0	0	0
737:	0	0	0	0	0	0	0	0
745:	1	0	0	0	0	0	0	0
753:	0	0	0	0	0	1	0	0
761:	0	0	0	0	0	0	0	1
769:	0	0	0	0	0	1	0	0
777:	0	0	0	0	0	0	0	0
785:	0	0	0	0	0	0	0	0
793:	0	0	0	0	0	0	0	0

Large Detector, Low Gain

***** S P E C T R A L D A T A R E P O R T *****

***** Sample ID: *****

Elapsed Live time: 14400

409:	0	0	0	0	0	0	0	0
417:	0	0	0	0	0	0	0	0
425:	0	0	0	0	0	0	0	0
433:	0	0	0	0	0	0	0	0
441:	0	0	0	0	0	0	0	0
449:	0	0	0	0	0	0	0	0
457:	0	0	0	0	0	0	0	0
465:	0	0	0	0	0	0	0	0
473:	0	0	0	0	0	0	0	0
481:	0	0	0	0	0	0	0	0
489:	0	0	0	0	0	0	0	0
497:	0	0	0	0	0	0	0	0
505:	0	0	0	0	0	0	0	0
513:	0	0	0	0	0	0	0	0
521:	0	0	0	0	0	0	0	0
529:	0	0	0	0	0	0	0	0
537:	0	0	0	0	0	0	0	0
545:	0	0	0	0	0	0	0	0
553:	0	0	0	0	0	0	1	0
561:	0	0	0	0	0	0	0	0
569:	0	0	0	0	0	0	0	0
577:	0	0	0	0	0	0	0	0
585:	0	0	0	0	0	0	0	0
593:	0	0	0	0	0	0	0	0
601:	0	0	0	0	0	0	0	0
609:	0	0	0	0	0	0	0	0
617:	0	0	0	0	0	0	0	0
625:	0	0	0	0	0	0	0	0
633:	0	0	0	0	0	0	0	0
641:	0	0	0	0	0	0	0	0
649:	0	0	0	0	0	0	0	0
657:	0	0	0	0	0	0	0	0
665:	0	0	0	0	0	0	0	0
673:	0	0	0	0	0	0	0	0
681:	0	0	0	0	0	0	0	0
689:	0	0	0	0	0	0	0	0
697:	0	0	0	0	0	0	0	0
705:	0	0	0	0	0	0	0	0
713:	0	0	0	0	0	0	0	0
721:	0	0	0	0	0	0	0	0
729:	0	0	0	0	0	0	0	0
737:	0	0	0	0	0	0	0	0
745:	0	0	0	0	0	0	0	0
753:	0	0	0	0	0	0	0	0
761:	0	0	0	0	0	0	0	0
769:	0	0	0	0	0	0	0	0
777:	0	0	0	0	0	0	0	0
785:	0	0	0	0	0	0	0	0
793:	0	0	0	0	0	0	0	0

Small Detector, High Gain

***** S P E C T R A L D A T A R E P O R T *****

***** Sample ID: *****

Elapsed Live time: 13592
 Elapsed Real Time: 14400

Channel	-----	-----	-----	-----	-----	-----	-----	-----	-----
1:	0	0	0	0	0	0	0	0	0
9:	0	0	0	0	0	0	1304	27361	
17:	484516	328413	203527	130793	88952	63596	45283	32811	
25:	23522	16490	11156	7465	4705	3023	1895	1233	
33:	735	481	344	224	179	129	101	77	
41:	59	42	34	26	20	31	17	13	
49:	13	9	11	14	9	6	3	7	
57:	1	5	3	3	2	4	1	3	
65:	0	6	2	1	1	0	2	0	
73:	0	1	0	1	1	2	2	3	
81:	0	1	1	1	0	0	0	0	
89:	0	0	0	1	2	0	0	0	
97:	1	2	1	0	0	1	1	0	
105:	0	0	0	0	1	1	2	1	
113:	0	0	2	0	2	0	0	0	
121:	0	1	0	0	0	1	0	0	
129:	0	0	0	0	1	0	1	0	
137:	1	1	0	0	0	0	0	0	
145:	0	1	1	1	0	0	0	1	
153:	0	0	0	0	0	0	0	1	
161:	0	1	0	0	0	0	0	1	
169:	0	0	1	0	0	0	0	1	
177:	0	0	0	0	0	0	0	0	
185:	0	0	0	0	0	0	1	0	
193:	0	0	0	0	0	0	0	0	
201:	0	0	2	0	0	0	0	0	
209:	0	0	0	0	0	0	0	0	
217:	0	0	0	0	0	0	0	0	1
225:	0	0	0	1	0	0	0	0	
233:	0	0	0	0	0	0	1	0	
241:	0	0	0	0	0	0	0	0	
249:	0	0	0	1	0	0	0	0	
257:	0	0	0	0	0	0	0	0	
265:	0	0	0	0	0	0	0	0	
273:	0	0	0	0	0	0	0	0	
281:	0	1	0	0	0	0	0	1	
289:	0	0	0	0	0	0	0	0	
297:	0	0	0	0	0	0	1	0	
305:	0	0	0	0	0	0	0	0	
313:	0	0	0	0	0	0	0	0	
321:	0	0	0	0	1	0	0	0	
329:	0	0	0	0	0	0	0	0	
337:	0	0	0	0	1	0	0	0	
345:	0	0	0	0	0	0	0	0	
353:	0	2	0	0	1	0	0	0	

361:	0	0	0	0	0	0	0
369:	0	0	0	0	0	0	0
377:	0	0	0	0	0	0	0
385:	0	0	0	0	1	0	0
393:	0	0	0	0	0	0	0
401:	0	0	0	0	0	0	0
409:	0	0	0	0	0	0	0
417:	0	0	0	0	0	0	0
425:	0	0	0	0	0	0	0
433:	1	0	0	0	0	0	0
441:	0	0	0	0	0	0	0
449:	0	0	0	0	0	0	0
457:	0	0	0	0	0	0	0
465:	0	0	0	0	0	0	0
473:	0	0	0	0	0	0	0
481:	0	0	0	0	0	0	0
489:	0	0	0	0	0	0	0
497:	0	0	0	0	0	0	0
505:	0	0	0	0	0	0	0
513:	0	0	0	0	1	0	0
521:	0	0	0	0	0	0	0
529:	0	0	0	0	0	0	0
537:	0	0	0	0	0	0	0
545:	0	0	0	0	0	0	0
553:	0	0	0	0	0	0	0
561:	0	0	0	0	0	0	0
569:	0	0	0	0	0	0	0
577:	0	0	0	0	0	0	0
585:	0	0	0	0	0	0	0
593:	0	0	0	0	0	0	0
601:	0	0	0	0	0	0	0
609:	0	0	0	0	0	0	0
617:	0	0	0	0	0	0	0
625:	0	0	0	0	0	0	0
633:	0	0	0	0	0	0	0
641:	0	0	0	0	0	0	0
649:	0	0	0	0	0	0	0
657:	0	0	0	0	0	0	0
665:	0	0	0	0	0	0	0
673:	0	0	0	0	0	0	0
681:	0	0	0	0	0	0	0
689:	0	0	0	0	0	0	0
697:	0	0	0	0	0	0	0
705:	0	0	0	0	0	0	0
713:	0	0	0	0	0	0	0
721:	0	0	0	0	0	0	0
729:	0	0	0	0	0	0	0
737:	0	0	0	0	0	0	0
745:	0	0	0	0	0	0	0
753:	0	0	0	0	0	0	0
761:	0	0	0	0	0	0	0
769:	0	0	0	0	0	0	0
777:	0	0	0	0	0	0	0
785:	0	0	0	0	0	0	0

793: 0 0 0 0 0 0 0 0 0

Small Detector, Low Gain

***** S P E C T R A L D A T A R E P O R T *****

***** Sample ID: *****

Elapsed Live time: 14394
Elapsed Real Time: 14400

313:	0	0	0	0	0	0	0
321:	0	0	0	0	0	0	0
329:	0	0	0	0	0	0	0
337:	0	0	0	0	0	0	0
345:	0	0	0	0	0	0	0
353:	0	0	0	0	0	0	0
361:	0	0	0	0	0	0	0
369:	0	0	0	0	0	0	0
377:	0	0	0	0	0	0	0
385:	0	0	0	0	0	0	0
393:	0	0	0	0	0	0	0
401:	0	0	0	0	0	0	0
409:	0	0	0	0	0	0	0
417:	0	0	0	0	0	0	0
425:	0	0	0	0	0	0	0
433:	0	0	0	0	0	0	0
441:	0	0	0	0	0	0	0
449:	0	0	0	0	0	0	0
457:	0	0	0	0	0	0	0
465:	0	0	0	0	0	0	0
473:	0	0	0	0	0	0	0
481:	0	0	0	0	0	0	0
489:	0	0	0	0	0	0	0
497:	0	0	0	0	0	0	0
505:	0	0	0	0	0	0	0
513:	0	0	0	0	0	0	0
521:	0	0	0	0	0	0	0
529:	0	0	0	0	0	0	0
537:	0	0	0	0	0	0	0
545:	0	0	0	0	0	0	0
553:	0	0	0	0	0	0	0
561:	0	0	0	0	0	0	0
569:	0	0	0	0	0	0	0
577:	0	0	0	0	0	0	0
585:	0	0	0	0	0	0	0
593:	0	0	0	0	0	0	0
601:	0	0	0	0	0	0	0
609:	0	0	0	0	0	0	0
617:	0	0	0	0	0	0	0
625:	0	0	0	0	0	0	0
633:	0	0	0	0	0	0	0
641:	0	0	0	0	0	0	0
649:	0	0	0	0	0	0	0
657:	0	0	0	0	0	0	0
665:	0	0	0	0	0	0	0
673:	0	0	0	0	0	0	0
681:	0	0	0	0	0	0	0
689:	0	0	0	0	0	0	0
697:	0	0	0	0	0	0	0
705:	0	0	0	0	0	0	0
713:	0	0	0	0	0	0	0
721:	0	0	0	0	0	0	0
729:	0	0	0	0	0	0	0
737:	0	0	0	0	0	0	0

745:	0	0	0	0	0	0	0	0
753:	0	0	0	0	0	0	0	0
761:	0	0	0	0	0	0	0	0
769:	0	0	0	0	0	0	0	0
777:	0	0	0	0	0	0	0	0
785:	0	0	0	0	0	0	0	0
793:	0	0	0	0	0	0	0	0

Section III: Data Set 3 for Am-Be neutron source with Plastic Shielding-4hrs

Large Detector, High Gain

***** S P E C T R A L D A T A R E P O R T *****

***** Sample ID: *****

Elapsed Live time: 11048
 Elapsed Real Time: 14400

Channel	-----	-----	-----	-----	-----	-----	-----	-----
1:	0	0	0	0	0	0	0	0
9:	1	0	0	0	0	0	627	4556
17:	*****	*****	*****	*****	8804112	7241290	5912399	4804238
25:	3892781	3139813	2522170	2020734	1616242	1286336	1023987	815816
33:	649502	513667	407661	324538	257690	205178	164423	131957
41:	106220	85795	69352	56457	46623	38533	31759	26747
49:	22655	19081	16662	14555	12897	11344	10120	9245
57:	8427	7621	7050	6644	6311	5850	5485	5142
65:	5011	4646	4418	4422	4235	4029	3791	3854
73:	3682	3536	3545	3435	3327	3188	3097	3087
81:	3002	2957	2906	2805	2682	2642	2639	2632
89:	2531	2359	2371	2380	2342	2249	2248	2203
97:	2205	2190	2004	2019	2044	1943	1891	1959
105:	1857	1843	1812	1795	1842	1750	1686	1673
113:	1650	1596	1682	1582	1543	1596	1563	1556
121:	1560	1494	1441	1460	1466	1348	1354	1398
129:	1327	1401	1354	1288	1253	1218	1254	1224
137:	1223	1204	1233	1149	1078	1171	1145	1167
145:	1109	1099	1051	1057	1112	1001	1076	1025
153:	1064	997	966	1017	945	968	915	985
161:	934	911	942	893	894	916	890	908
169:	912	896	905	892	807	873	849	886
177:	821	838	841	827	814	816	780	748
185:	713	741	711	760	733	727	729	770
193:	684	743	676	708	716	687	704	664
201:	666	720	675	650	709	669	674	649
209:	646	603	633	651	664	587	665	656
217:	619	646	571	623	610	617	608	561

225:	588	605	541	556	558	576	575	529
233:	543	549	527	551	546	550	522	545
241:	500	487	521	537	496	520	520	532
249:	495	509	537	505	534	506	482	518
257:	473	453	477	473	461	440	512	495
265:	460	479	495	459	506	444	441	456
273:	444	453	409	455	481	436	462	445
281:	427	452	426	419	407	443	382	424
289:	406	436	417	395	417	384	471	433
297:	411	427	387	381	371	428	384	352
305:	373	405	363	352	385	357	343	364
313:	380	374	353	353	358	384	362	337
321:	358	360	352	358	344	326	349	344
329:	333	319	308	328	342	343	341	317
337:	271	325	296	292	301	325	310	313
345:	315	331	297	277	320	317	287	299
353:	315	291	311	289	257	298	315	259
361:	289	279	281	288	288	262	278	270
369:	285	260	282	269	281	256	261	274
377:	255	240	237	276	257	244	242	248
385:	265	271	235	207	270	228	231	222
393:	246	214	227	235	240	244	235	221
401:	237	214	242	252	240	216	237	246
409:	204	205	217	235	245	208	190	203
417:	214	206	219	213	215	199	219	232
425:	190	184	217	190	185	207	184	180
433:	202	191	189	188	193	189	170	180
441:	186	209	179	181	157	174	178	178
449:	181	189	177	189	181	182	158	182
457:	185	172	151	184	175	162	169	140
465:	153	183	186	174	141	161	147	155
473:	163	126	162	152	137	148	157	141
481:	149	140	156	131	142	133	143	137
489:	134	127	131	117	134	143	148	150
497:	165	125	153	113	137	123	132	121
505:	132	136	134	120	121	128	104	126
513:	127	114	118	118	109	108	130	104
521:	100	126	109	95	120	108	103	107
529:	98	115	125	105	111	106	104	105
537:	112	98	79	97	93	112	92	98
545:	92	98	75	106	88	79	89	99
553:	89	88	98	87	88	99	98	85
561:	90	76	85	77	101	78	72	82
569:	94	87	91	83	109	75	92	76
577:	82	89	80	71	75	76	90	73
585:	80	75	79	73	85	78	74	75
593:	76	86	71	73	73	87	88	79
601:	58	68	69	74	70	64	62	75
609:	67	73	66	63	68	67	68	73
617:	72	54	58	70	63	57	69	58
625:	64	67	68	69	67	68	60	64
633:	65	81	62	51	68	60	61	58
641:	53	57	71	56	56	66	56	65
649:	60	68	55	53	68	60	64	69

657:	63	69	48	52	69	51	62	50
665:	63	63	56	56	60	65	54	52
673:	52	55	58	51	56	51	63	70
681:	50	55	40	60	61	63	57	61
689:	56	56	53	55	41	55	62	39
697:	48	51	49	48	45	39	50	53
705:	54	54	52	49	50	47	56	44
713:	51	48	55	40	48	49	45	47
721:	43	44	54	40	46	39	43	46
729:	45	41	52	47	35	43	48	41
737:	52	49	44	49	48	34	50	51
745:	47	37	36	32	48	46	34	46
753:	48	45	44	49	57	43	47	36
761:	59	37	38	35	43	44	33	46
769:	44	50	46	39	38	54	35	43
777:	48	42	43	51	41	43	38	46
785:	45	39	53	50	38	57	33	40
793:	43	44	29	33	41	43	49	33

Large Detector, Low Gain

***** S P E C T R A L D A T A R E P O R T *****

***** Sample ID: *****

Elapsed Live time: 14399
 Elapsed Real Time: 14400

Channel	-----	-----	-----	-----	-----	-----	-----	-----
1:	0	0	0	0	0	0	0	0
9:	0	0	0	0	0	0	0	8
17:	1898	1826	1763	1623	1476	1442	1467	1312
25:	1197	1131	1091	950	919	883	851	807
33:	768	704	627	603	585	645	573	524
41:	466	449	458	393	414	383	388	380
49:	321	300	296	280	306	261	269	225
57:	234	216	208	182	201	175	190	155
65:	137	171	128	154	143	149	150	125
73:	120	129	120	115	94	95	115	90
81:	99	81	96	100	91	86	95	83
89:	68	80	75	60	66	64	71	86
97:	67	59	63	54	51	64	48	70
105:	44	56	47	54	53	37	45	52
113:	48	42	35	47	54	41	40	46
121:	31	38	40	36	30	33	28	29
129:	27	30	33	20	28	32	36	32
137:	27	31	21	24	29	23	32	21
145:	25	18	21	24	25	18	23	18
153:	24	16	21	18	27	14	23	16
161:	20	14	11	19	14	13	13	11
169:	17	13	13	18	13	8	13	11

177:	4	11	12	16	8	6	10	5
185:	5	5	7	11	3	6	8	4
193:	8	2	6	4	7	6	5	6
201:	5	6	4	5	7	12	6	6
209:	5	4	3	3	3	7	2	3
217:	3	1	5	3	4	4	10	1
225:	4	5	3	3	2	2	2	5
233:	1	0	3	2	3	5	2	1
241:	4	5	2	5	2	3	3	2
249:	1	2	4	3	1	6	3	2
257:	5	1	5	4	0	1	3	1
265:	1	0	4	2	1	2	2	1
273:	2	2	1	3	4	2	2	2
281:	1	3	0	2	3	3	6	1
289:	2	3	1	2	1	2	2	2
297:	1	4	2	1	4	0	2	2
305:	1	1	2	1	3	1	0	0
313:	3	3	2	2	1	3	1	1
321:	2	3	2	3	2	1	0	2
329:	0	5	0	1	0	1	1	1
337:	1	2	0	1	4	1	1	1
345:	1	2	0	1	4	2	0	3
353:	3	1	1	1	1	0	0	0
361:	2	1	2	0	0	1	1	2
369:	0	0	0	0	1	3	1	1
377:	1	0	4	1	2	2	1	1
385:	0	1	1	3	0	0	3	1
393:	1	2	0	1	3	0	4	2
401:	0	2	1	0	0	0	0	2
409:	1	1	1	0	2	1	2	1
417:	1	0	1	0	0	1	1	1
425:	1	0	0	1	0	1	1	0
433:	3	0	2	1	2	0	1	1
441:	0	1	0	1	0	1	1	0
449:	1	0	0	1	0	0	2	1
457:	1	1	1	0	0	0	0	1
465:	0	0	2	0	1	1	2	1
473:	1	1	0	1	0	0	0	0
481:	3	0	0	1	1	0	1	1
489:	0	0	1	0	0	0	0	0
497:	0	0	0	2	0	0	0	0
505:	0	0	1	0	2	0	1	0
513:	0	3	0	0	0	2	0	1
521:	0	1	2	0	0	0	1	0
529:	0	0	0	0	0	0	0	0
537:	1	1	2	1	0	0	0	0
545:	0	3	0	0	0	0	1	0
553:	0	0	0	0	0	2	0	0
561:	0	1	2	0	0	0	2	0
569:	0	2	0	0	0	1	0	0
577:	0	2	0	1	1	1	0	1
585:	0	0	0	0	1	0	0	0
593:	0	0	1	0	0	1	0	1
601:	0	0	1	1	0	0	1	0

609:	0	0	1	0	0	1	0	1
617:	1	0	0	0	0	0	0	0
625:	0	0	0	0	0	0	0	1
633:	0	0	0	1	1	0	0	0
641:	0	0	0	0	0	0	1	0
649:	0	0	0	0	0	0	0	0
657:	0	1	2	0	1	0	0	0
665:	0	1	0	2	0	0	0	0
673:	0	0	0	0	0	1	0	0
681:	0	0	0	0	0	1	0	0
689:	0	0	0	1	0	0	1	1
697:	0	0	0	0	0	0	1	1
705:	0	0	0	0	1	0	0	0
713:	0	0	1	1	0	0	0	0
721:	0	0	0	0	0	1	0	0
729:	0	0	0	0	0	0	0	0
737:	0	0	0	1	0	0	0	0
745:	1	1	0	0	0	0	0	1
753:	0	0	1	0	0	0	0	0
761:	0	0	0	0	0	0	0	0
769:	0	0	0	0	0	0	0	0
777:	0	0	0	0	0	0	0	0
785:	0	0	0	0	1	0	0	0
793:	0	0	0	0	0	0	0	0

Small Detector, High Gain

***** S P E C T R A L D A T A R E P O R T *****

***** Sample ID: *****

Elapsed Live time: 11544
 Elapsed Real Time: 14400

Channel	-----	-----	-----	-----	-----	-----	-----	-----
1:	0	0	0	0	0	0	0	0
9:	0	0	0	0	0	7	26549	640909
17:	8950408	7777295	6097027	4700189	3575488	2683971	1989366	1466240
25:	1074592	788117	579933	430225	325905	250602	198838	160088
33:	132855	111952	94690	82037	70627	61125	52987	45590
41:	39561	34130	28900	24616	20852	17460	14327	11778
49:	9620	7753	6171	4836	3946	3073	2462	1954
57:	1528	1319	1132	909	769	697	638	551
65:	511	477	435	387	398	357	356	350
73:	278	322	265	299	289	339	240	266
81:	267	217	229	242	208	212	197	238
89:	214	214	213	201	196	180	166	183
97:	180	174	178	183	194	143	160	154
105:	147	186	143	146	158	131	153	158
113:	122	104	132	148	136	117	140	133
121:	104	116	108	104	129	116	121	115

129:	112	104	91	113	95	99	110	110
137:	104	95	107	92	101	111	101	101
145:	92	110	96	94	86	76	81	86
153:	96	79	83	84	78	93	70	75
161:	65	71	68	87	86	76	68	84
169:	79	80	57	65	62	75	70	63
177:	68	60	62	47	73	53	61	76
185:	65	83	69	59	63	59	49	69
193:	63	76	60	56	52	49	65	48
201:	53	49	51	76	61	58	53	53
209:	67	53	55	53	66	51	56	56
217:	41	42	47	59	51	54	41	53
225:	45	57	43	58	60	47	52	40
233:	48	51	45	44	49	41	42	42
241:	44	52	40	35	37	40	47	34
249:	49	35	48	44	33	48	48	33
257:	39	30	36	41	34	39	45	50
265:	35	37	27	40	47	38	38	40
273:	33	46	30	39	47	34	27	32
281:	35	34	37	35	38	28	29	29
289:	32	34	38	31	26	37	35	30
297:	31	34	32	36	32	27	33	21
305:	28	40	27	34	36	29	37	30
313:	44	32	28	28	33	26	26	29
321:	27	21	25	28	24	17	20	33
329:	21	22	35	33	25	34	22	22
337:	27	20	19	28	29	21	22	20
345:	27	37	22	27	20	23	22	24
353:	25	18	16	25	21	18	35	24
361:	28	18	24	20	18	25	18	16
369:	20	28	25	16	15	18	15	18
377:	16	19	20	22	16	19	13	14
385:	24	22	19	19	19	19	17	21
393:	18	13	13	14	19	17	17	20
401:	18	13	16	18	16	21	22	17
409:	16	13	18	20	15	14	15	19
417:	15	12	20	14	13	12	17	21
425:	17	18	16	15	16	19	9	12
433:	20	19	16	15	13	18	6	21
441:	13	11	17	9	12	11	11	12
449:	14	9	12	16	12	7	11	24
457:	15	12	15	12	16	14	13	10
465:	11	15	11	13	5	11	8	10
473:	12	15	12	12	11	13	14	15
481:	13	10	8	10	9	18	10	17
489:	7	11	4	11	9	11	12	5
497:	12	9	11	8	11	11	8	15
505:	9	6	5	15	10	5	6	12
513:	11	15	6	9	10	8	12	5
521:	5	9	5	11	10	4	9	6
529:	6	10	11	13	9	4	10	4
537:	13	11	9	1	3	13	8	13
545:	9	9	9	12	7	4	12	11
553:	8	8	8	14	6	8	4	8

561:	4	11	6	5	4	10	8	9
569:	10	5	8	11	3	4	13	9
577:	7	9	5	8	3	17	8	7
585:	8	7	8	3	4	7	9	4
593:	12	12	7	11	4	4	10	12
601:	7	1	9	10	6	8	5	7
609:	8	4	8	7	9	7	7	6
617:	4	7	3	7	4	7	7	2
625:	9	7	6	5	4	5	8	5
633:	6	4	2	11	6	6	9	3
641:	7	7	6	13	7	3	6	7
649:	4	5	6	11	7	5	3	7
657:	7	2	7	3	5	5	11	7
665:	4	3	7	10	5	11	8	8
673:	6	8	8	8	5	4	6	8
681:	1	3	2	4	5	11	2	3
689:	4	7	7	4	4	4	5	7
697:	5	8	8	5	7	9	1	7
705:	7	3	1	1	8	4	1	4
713:	3	5	5	3	2	1	2	3
721:	3	6	2	5	8	7	6	7
729:	3	3	4	4	9	4	7	6
737:	4	4	4	6	1	6	6	5
745:	5	5	1	3	9	2	6	4
753:	4	8	2	5	6	7	7	6
761:	1	3	7	4	8	5	6	4
769:	0	4	2	5	4	4	7	4
777:	4	5	2	2	2	5	0	2
785:	1	4	4	4	4	3	1	5
793:	7	2	3	7	9	1	2	3

Small Detector, Low Gain

***** S P E C T R A L D A T A R E P O R T *****

***** Sample ID: *****

Elapsed Live time: 14336
 Elapsed Real Time: 14400

Channel	-----	-----	-----	-----	-----	-----	-----	-----
1:	79	493	1065	1184	1010	923	935	908
9:	825	779	724	626	559	529	409	383
17:	357	316	276	239	205	201	198	188
25:	150	142	159	137	108	113	120	84
33:	97	79	77	88	76	75	82	61
41:	55	55	51	41	50	46	51	47
49:	39	40	53	46	39	32	30	27
57:	28	24	35	36	25	35	27	19
65:	17	23	29	27	23	21	11	12

505:	1	0	0	0	0	0	0	0
513:	0	0	0	0	0	0	0	0
521:	0	0	0	0	1	0	0	0
529:	0	0	0	0	0	0	0	0
537:	0	0	0	0	0	0	0	0
545:	0	0	0	0	0	0	0	0
553:	0	0	0	0	0	0	0	0
561:	0	0	0	0	0	0	0	0
569:	0	0	0	0	0	0	0	0
577:	0	0	0	0	0	0	0	0
585:	0	0	0	0	0	0	0	0
593:	0	0	0	0	0	0	0	0
601:	0	0	0	0	0	0	0	0
609:	0	0	0	0	0	0	0	0
617:	0	0	0	0	0	0	0	0
625:	0	0	0	0	0	1	0	0
633:	0	0	0	0	0	0	0	0
641:	0	0	0	0	0	0	0	0
649:	0	0	0	0	0	0	0	0
657:	0	0	0	0	0	0	0	0
665:	0	0	0	0	0	0	0	0
673:	0	0	0	0	0	0	0	0
681:	0	0	0	1	0	0	0	0
689:	0	0	0	0	0	1	0	0
697:	0	0	0	0	0	0	0	0
705:	0	0	0	0	0	0	0	0
713:	0	0	0	0	0	0	0	0
721:	0	0	0	0	0	0	0	0
729:	0	0	0	0	0	0	0	0
737:	0	0	0	0	0	1	0	0
745:	0	0	0	0	0	0	0	0
753:	0	0	0	0	0	0	0	0
761:	0	0	0	0	0	0	0	0
769:	0	0	0	0	0	0	0	0
777:	0	0	0	0	0	0	0	0
785:	0	0	0	0	0	0	0	0
793:	0	0	0	0	0	0	0	0

Section IV: Data Set 4 for Am-Be neutron source with Plastic Shielding-24hrs

Large Detector, High Gain

```
*****
***** S P E C T R A L D A T A R E P O R T *****
*****
```

```
***** Sample ID: *****
```

Elapsed Live time: 43322
 Elapsed Real Time: 53999

Channel										
1:	0	0	0	0	0	0	0	0	0	0
9:	6	0	0	0	0	0	0	2078	23522	
17:	*****	*****	*****	*****	*****	*****	*****	*****	*****	8646814
25:	6586258	4998934	3776726	2851481	2145915	1616190	1218638	921920		
33:	703316	538624	417345	329679	264490	216181	179760	153779		
41:	133795	118172	106641	96824	88682	81523	74961	68743		
49:	63658	58719	53569	48809	44361	40584	37159	33607		
57:	30952	28452	26390	24426	22390	21197	19950	18897		
65:	17932	16999	16181	15880	14941	14420	13915	13594		
73:	13169	12788	12664	12246	12085	11842	11423	11125		
81:	11172	10690	10578	10466	10199	9832	9673	9390		
89:	9180	9124	8846	8937	8634	8457	8400	8221		
97:	7964	8024	7869	7580	7524	7575	7129	7151		
105:	7005	6786	6867	6574	6581	6579	6423	6402		
113:	6193	6077	6133	5989	5701	5799	5661	5702		
121:	5743	5386	5540	5367	5157	5155	4953	5039		
129:	5019	4967	4961	4654	4757	4749	4677	4633		
137:	4543	4578	4344	4335	4358	4328	4365	4357		
145:	4233	4257	4047	3977	3908	3921	3911	3818		
153:	3822	3753	3679	3735	3739	3541	3681	3600		
161:	3341	3537	3488	3452	3396	3271	3434	3313		
169:	3306	3300	3270	3162	3227	3186	3197	3101		
177:	3031	3088	3019	3071	2901	2972	2931	2952		
185:	2990	2961	2840	2864	2734	2879	2785	2874		
193:	2679	2667	2685	2749	2743	2617	2608	2616		
201:	2491	2576	2528	2513	2412	2460	2378	2438		
209:	2414	2438	2326	2450	2461	2387	2351	2269		
217:	2240	2293	2256	2254	2246	2172	2254	2182		
225:	2204	2260	2178	2211	2088	2149	2164	2077		
233:	2066	2090	2079	2095	2009	1991	2066	2074		
241:	1967	2050	1942	2007	1944	1935	1926	1888		
249:	1936	1853	1850	1897	1833	1894	1801	1830		
257:	1825	1875	1831	1879	1756	1734	1746	1777		
265:	1784	1712	1745	1668	1752	1704	1731	1673		
273:	1671	1678	1670	1670	1668	1632	1606	1570		
281:	1608	1603	1543	1525	1501	1563	1550	1541		
289:	1531	1463	1475	1563	1445	1500	1482	1491		
297:	1524	1472	1496	1510	1461	1529	1399	1416		
305:	1410	1431	1484	1336	1439	1408	1375	1307		
313:	1348	1346	1338	1324	1384	1352	1323	1293		
321:	1278	1288	1280	1259	1289	1274	1253	1197		
329:	1296	1238	1271	1160	1299	1199	1233	1230		
337:	1200	1207	1205	1219	1185	1187	1125	1208		
345:	1124	1190	1122	1152	1105	1091	1147	1160		
353:	1130	1101	1129	1153	1124	1056	1064	1138		
361:	1074	1077	1079	1062	1106	1061	1026	1154		
369:	1073	1071	1006	994	1018	1041	1012	1030		
377:	1023	929	1020	1005	966	950	989	961		
385:	969	923	959	950	926	891	848	907		
393:	847	904	913	937	920	857	911	870		

401:	857	873	898	851	849	852	813	861
409:	826	863	846	817	816	831	777	825
417:	792	770	774	787	815	812	784	789
425:	776	728	747	730	729	771	756	742
433:	759	766	764	773	729	723	682	691
441:	711	662	681	652	655	650	709	648
449:	678	692	651	641	658	658	676	642
457:	695	634	588	627	613	629	631	600
465:	636	643	604	567	626	587	579	635
473:	646	573	602	558	565	592	547	576
481:	508	566	576	523	569	526	543	522
489:	548	474	535	517	561	503	509	522
497:	493	516	438	471	480	485	482	497
505:	515	472	447	466	437	477	500	439
513:	497	447	465	469	443	446	421	436
521:	443	437	431	426	425	490	449	420
529:	455	402	391	428	438	421	424	383
537:	374	432	402	394	395	367	402	360
545:	345	366	369	347	380	381	352	352
553:	385	365	337	342	358	331	350	337
561:	345	374	324	349	318	336	307	298
569:	326	315	330	321	323	311	301	298
577:	313	297	288	303	312	300	287	321
585:	318	280	291	313	289	285	274	302
593:	262	291	288	282	272	287	268	277
601:	261	295	291	296	278	266	259	277
609:	258	277	278	291	264	269	290	241
617:	261	246	262	273	255	265	230	239
625:	282	206	220	222	220	255	259	234
633:	243	225	233	227	249	228	245	239
641:	241	256	253	244	225	230	239	225
649:	229	232	217	218	224	205	232	235
657:	217	241	172	204	219	206	213	199
665:	212	195	208	186	219	173	221	214
673:	202	233	183	214	232	202	201	205
681:	196	220	196	210	194	199	210	178
689:	189	201	177	191	185	180	179	180
697:	212	201	189	189	189	177	224	181
705:	174	173	180	182	199	211	170	179
713:	186	193	192	195	182	172	184	185
721:	177	206	198	173	179	171	223	176
729:	170	164	201	172	151	184	177	167
737:	202	160	178	145	171	155	188	164
745:	165	179	167	203	170	173	170	154
753:	158	147	148	156	140	147	166	156
761:	202	168	171	175	174	168	157	173
769:	160	164	160	151	162	168	159	160
777:	168	140	162	151	162	159	174	144
785:	148	167	143	157	161	167	145	178
793:	155	151	159	168	171	153	156	167

Large Detector, Low Gain

```
*****
***** S P E C T R A L D A T A R E P O R T *****
*****
```

```
***** Sample ID: *****
```

```
Elapsed Live time: 53996
Elapsed Real Time: 53999
```

Channel	-----	-----	-----	-----	-----	-----	-----	-----
1:	0	0	0	0	0	0	0	0
9:	0	0	0	0	0	0	0	64
17:	6850	6791	6469	5975	5606	5282	5075	4749
25:	4421	4225	3911	3814	3579	3312	3244	3006
33:	2831	2701	2494	2376	2252	2018	2031	1897
41:	1772	1670	1668	1572	1419	1393	1299	1293
49:	1190	1225	1102	1013	1034	935	917	933
57:	896	823	785	746	687	759	677	652
65:	620	593	604	604	531	528	523	509
73:	451	505	449	413	397	415	393	398
81:	407	361	346	327	299	325	313	295
89:	310	272	265	280	246	275	269	254
97:	263	246	280	228	225	219	187	218
105:	201	203	213	208	188	175	188	146
113:	152	185	163	167	156	136	145	167
121:	150	138	138	133	122	126	121	124
129:	117	118	112	123	98	110	116	99
137:	120	103	105	95	77	84	88	96
145:	96	80	86	87	87	86	79	86
153:	71	86	67	81	67	66	69	69
161:	54	47	52	61	65	48	50	47
169:	50	50	49	39	41	39	36	35
177:	32	41	39	32	35	37	34	33
185:	25	24	31	22	30	28	31	23
193:	20	19	29	26	27	16	25	9
201:	23	16	13	13	11	13	14	14
209:	24	17	9	12	16	5	16	4
217:	16	9	7	14	2	12	10	8
225:	5	8	12	11	12	14	8	6
233:	7	7	7	11	12	14	10	3
241:	11	10	9	12	3	7	12	8
249:	13	8	6	10	5	9	6	11
257:	14	13	5	7	9	10	7	11
265:	5	9	8	10	5	11	8	10
273:	10	9	8	6	5	5	8	16
281:	6	4	7	5	8	12	9	4
289:	7	3	6	6	7	8	4	11
297:	9	6	8	7	10	6	9	3
305:	3	7	4	8	6	4	4	3
313:	5	6	5	6	7	2	5	5

321:	3	8	6	7	3	6	8	2
329:	5	4	6	5	4	3	5	5
337:	11	8	7	7	4	3	1	4
345:	6	7	5	4	5	6	5	5
353:	5	7	4	3	6	7	4	2
361:	7	2	4	4	6	4	4	2
369:	3	4	3	4	3	5	1	0
377:	2	3	2	3	1	3	4	3
385:	8	3	3	1	3	2	4	2
393:	5	6	3	5	3	3	2	4
401:	5	4	1	2	1	4	3	3
409:	3	2	5	5	5	6	6	4
417:	2	1	1	1	1	3	3	3
425:	0	3	3	3	0	5	1	5
433:	2	5	3	3	5	2	3	6
441:	3	5	3	6	10	1	3	2
449:	6	2	1	3	4	1	3	1
457:	4	5	3	6	1	5	6	3
465:	2	2	6	5	2	1	1	1
473:	5	1	2	3	1	1	2	1
481:	4	2	4	3	1	3	4	1
489:	3	1	3	2	1	1	6	0
497:	2	3	2	1	2	1	0	6
505:	1	1	3	4	0	1	2	1
513:	1	2	5	3	2	0	2	4
521:	2	3	1	2	2	1	2	3
529:	0	1	1	4	4	6	2	1
537:	1	3	0	3	0	1	1	3
545:	5	2	0	1	1	1	1	2
553:	3	1	2	0	5	2	3	3
561:	2	2	1	0	0	1	2	2
569:	0	1	3	1	3	1	1	2
577:	5	3	2	3	1	1	1	0
585:	0	5	0	0	1	2	0	0
593:	2	2	1	2	1	1	4	0
601:	0	0	1	1	2	2	1	1
609:	0	0	1	2	0	2	1	0
617:	1	2	0	0	0	0	1	0
625:	0	1	2	1	1	0	1	1
633:	1	2	0	2	2	3	0	0
641:	1	2	1	4	0	0	1	0
649:	0	1	0	2	3	0	0	1
657:	0	2	1	0	2	0	1	2
665:	2	0	1	1	1	0	1	0
673:	0	0	1	3	1	1	0	1
681:	3	0	0	0	0	2	0	0
689:	2	0	1	0	1	0	1	1
697:	1	0	1	1	1	1	0	0
705:	0	2	2	1	1	1	1	1
713:	0	0	1	0	0	0	1	0
721:	1	0	0	0	1	2	1	0
729:	1	0	1	0	1	1	1	1
737:	0	1	0	1	0	1	0	0
745:	0	0	0	1	1	1	0	0

753:	0	1	2	0	2	2	0	1
761:	0	0	0	1	0	1	0	0
769:	1	1	2	0	1	2	0	0
777:	1	0	0	0	0	1	0	2
785:	0	2	0	1	1	0	2	1
793:	1	0	1	0	0	0	0	0

Small Detector, High Gain

 ***** S P E C T R A L D A T A R E P O R T *****

***** Sample ID: *****

Elapsed Live time: 50118
 Elapsed Real Time: 54000

Channel	-----	-----	-----	-----	-----	-----	-----	-----
1:	0	0	0	0	0	0	0	0
9:	0	0	0	0	0	15	16748	372413
17:	4431606	3079643	1998622	1295357	842592	545713	356050	231539
25:	152048	101793	69408	48386	34880	26028	19791	15423
33:	12091	9798	7912	6413	5520	4794	4249	3693
41:	3417	3181	3000	2818	2688	2520	2478	2255
49:	2156	2095	2091	2013	1921	1797	1793	1741
57:	1738	1698	1628	1567	1512	1514	1401	1401
65:	1370	1369	1225	1316	1227	1162	1085	1150
73:	1100	1017	1074	1076	986	997	961	945
81:	929	907	835	827	897	863	844	780
89:	784	786	730	737	730	670	753	712
97:	678	653	672	620	602	620	628	612
105:	574	576	580	557	547	537	545	549
113:	524	527	514	503	497	530	474	478
121:	475	461	428	481	438	419	497	427
129:	397	427	426	423	422	412	383	382
137:	397	369	400	356	364	373	375	368
145:	359	323	360	347	363	357	318	315
153:	320	316	289	306	357	329	314	313
161:	284	322	278	272	282	274	279	271
169:	283	254	286	298	241	297	279	263
177:	251	267	265	257	256	249	229	210
185:	241	241	232	233	250	226	247	238
193:	242	253	234	228	254	258	208	220
201:	233	196	213	235	199	193	194	220
209:	197	202	230	193	209	193	189	197
217:	183	203	180	186	188	198	188	207
225:	181	188	198	206	173	171	170	178
233:	158	167	174	156	163	165	167	176
241:	171	158	176	157	139	155	161	167
249:	168	154	173	167	133	145	189	152
257:	147	161	138	145	144	153	153	143

265:	143	138	129	139	131	145	140	129
273:	142	142	126	130	131	126	147	140
281:	139	148	141	122	132	125	113	149
289:	146	121	129	122	119	126	107	129
297:	117	123	116	113	136	110	128	111
305:	128	113	103	98	115	107	113	113
313:	136	113	128	110	106	109	96	104
321:	85	97	101	114	101	100	93	112
329:	106	94	99	94	115	93	106	104
337:	89	107	112	100	109	76	89	85
345:	90	108	112	92	87	81	103	86
353:	86	92	84	92	73	87	81	99
361:	92	51	83	92	76	90	73	98
369:	77	83	94	73	69	77	77	72
377:	81	69	72	72	79	68	61	81
385:	77	92	77	72	74	84	83	71
393:	73	71	77	61	68	64	67	73
401:	59	70	69	63	71	55	74	54
409:	64	60	77	57	64	71	74	81
417:	63	68	52	68	51	66	61	66
425:	50	60	58	53	55	67	49	62
433:	56	59	49	45	59	64	65	49
441:	74	45	53	60	59	49	51	46
449:	54	60	51	46	60	53	43	51
457:	42	48	52	44	47	43	51	51
465:	53	69	41	38	37	40	43	50
473:	48	53	48	50	54	42	62	32
481:	56	55	45	51	47	49	38	43
489:	46	50	41	42	53	54	46	38
497:	42	34	33	52	35	25	39	30
505:	45	45	40	39	30	38	45	43
513:	47	42	49	40	37	35	35	52
521:	37	30	39	35	39	34	32	41
529:	37	35	36	30	55	34	40	32
537:	41	28	36	26	31	31	44	41
545:	27	39	31	27	29	32	29	29
553:	33	38	22	28	36	30	34	31
561:	23	35	37	29	27	28	32	32
569:	30	26	24	40	37	43	25	29
577:	33	27	32	33	29	22	32	27
585:	39	34	35	25	26	22	29	33
593:	29	26	30	37	31	37	34	18
601:	27	26	16	18	27	35	27	28
609:	18	24	27	21	27	28	18	24
617:	30	22	29	37	16	23	18	25
625:	22	25	28	23	28	17	26	25
633:	23	22	23	28	27	22	34	14
641:	28	22	30	24	34	24	32	18
649:	39	25	22	29	24	26	18	25
657:	34	27	23	24	21	27	39	22
665:	29	19	24	13	25	28	17	22
673:	17	27	25	28	18	17	24	17
681:	19	27	25	22	25	10	22	14
689:	23	28	21	24	24	19	14	26

697:	24	22	11	18	20	19	13	26
705:	16	22	17	22	23	26	16	19
713:	20	15	25	17	23	19	18	20
721:	11	19	22	11	18	25	17	13
729:	12	21	19	15	20	15	17	15
737:	21	16	21	14	16	17	18	16
745:	16	16	19	20	18	13	18	26
753:	15	21	16	20	18	19	21	18
761:	17	17	15	16	16	13	19	21
769:	15	15	17	18	19	14	15	23
777:	17	18	15	28	11	19	11	22
785:	18	21	19	17	13	14	11	24
793:	21	18	15	10	14	18	15	11

Small Detector, Low Gain

***** S P E C T R A L D A T A R E P O R T *****

***** Sample ID: *****

Elapsed Live time: 53950
Elapsed Real Time: 54000

209:	3	3	2	1	1	4	4	1
217:	2	2	1	1	2	2	0	2
225:	3	3	1	0	1	2	3	2
233:	2	4	3	2	1	3	0	2
241:	1	1	2	2	0	3	3	2
249:	2	2	1	0	1	1	0	1
257:	2	1	1	0	0	1	0	0
265:	2	1	0	1	1	0	1	2
273:	2	1	0	1	2	2	2	1
281:	1	3	0	1	2	1	5	0
289:	0	1	0	0	1	0	0	0
297:	0	0	2	0	1	2	0	1
305:	0	1	0	0	0	2	0	0
313:	2	1	0	0	0	1	1	0
321:	1	1	2	0	1	0	0	0
329:	0	3	0	0	1	0	2	0
337:	0	0	2	0	1	0	0	0
345:	1	0	0	1	1	0	0	1
353:	2	0	0	1	1	0	0	2
361:	0	0	0	0	1	4	2	0
369:	0	1	2	3	1	1	0	0
377:	0	1	0	0	1	0	0	0
385:	0	0	1	1	0	0	0	0
393:	0	1	1	0	0	0	1	0
401:	0	0	0	0	0	0	2	0
409:	0	0	0	3	0	1	0	0
417:	0	1	0	0	0	0	1	0
425:	1	1	0	0	0	0	1	1
433:	0	0	1	0	2	1	1	0
441:	0	1	0	0	0	0	1	0
449:	0	0	1	0	0	0	0	0
457:	2	0	1	0	0	0	0	0
465:	0	2	0	1	0	0	0	1
473:	0	0	0	1	0	0	0	0
481:	0	0	0	0	0	0	0	1
489:	0	0	0	1	0	1	0	0
497:	0	0	1	0	0	0	0	0
505:	0	0	0	0	0	0	0	0
513:	0	0	1	0	0	1	0	1
521:	0	0	0	0	0	0	0	0
529:	0	0	0	0	0	0	0	0
537:	0	0	0	0	0	0	0	0
545:	0	0	0	1	0	0	0	0
553:	0	0	0	1	0	0	0	0
561:	0	0	0	0	0	1	0	0
569:	0	0	0	0	0	0	0	0
577:	0	0	0	0	1	0	0	0
585:	0	0	0	0	0	0	0	0
593:	0	1	0	0	0	0	0	1
601:	0	0	0	0	0	0	0	0
609:	0	0	0	1	0	0	0	0
617:	0	0	0	0	0	0	0	1
625:	0	1	0	1	0	0	0	1
633:	1	0	0	0	1	0	0	0

VITA

Zhenghua Xia received her Bachelor of Engineering degree in nuclear engineering from Tsinghua University, China in 2001. She entered the health physics program at the University of Cincinnati in September 2003 and received her Master of Science degree in major subject August 2004. She received her Ph.D. degree in nuclear engineering from Texas A&M University in December 2008. Her research interests include radiation detection, radiation protection and medical physics.

Ms. Xia may be reached at the Nuclear Engineering Department, Texas A&M University, College Station, TX 77843-3133. Her email address is xiazhenghuacn@yahoo.com.cn.